

**Bandwidth Enhancement  
in  
Microstrip Antennas**

**Project Report**

Submitted in partial fulfillment of the requirement for  
the degree of  
**Bachelor of Technology**

**By**

**Ksh. Rakhesh Singh  
96007032**

**Under the guidance  
of  
Prof. Girish Kumar**



Department of Electrical Engineering  
Indian Institute of Technology  
Bombay  
April 2000

## Project approval sheet

Project titled "**Bandwidth Enhancement in Microstrip Antennas**"  
by Ksh. Rakesh Singh is approved for the degree of **Bachelor of Technology**  
in Electrical Engineering.

**Guide**

---

**Internal Examiner**

---

**External examiner**

---

**Chairman**

---

## Acknowledgement

I would like to express my sincere gratitude towards all people who have been instrumental in completing this project.

First and foremost, I am indebted to my guide, Prof. Girish Kumar, Dept. of Electrical Engineering, I.I.T-Bombay, for his invaluable guidance, encouragement and help. He inspired me to become a better researcher.

I am also indebted to Amit A. Deshmukh and Viswanatha Reddy. It would have been difficult to accomplish this project without their assistance and suggestions.

Last but not the least, I express my sincere thanks to each and everyone at the Microwave lab, Electrical Engineering, I.I.T-Bombay, for their assistance.

*Ksh. Rakesh Singh*  
(96007032)

## **Abstract**

Narrow bandwidth has been one of the most serious limitations hindering the wider applications of the microstrip antenna technology. For this reason, much of the research and development in microstrip antennas has been devoted to various techniques for the enhancement of the antenna bandwidth. But, most of these techniques, either increases the thickness or lateral size of the antenna. An antenna with U-slot needs no additional structure and gives a bandwidth greater than 30%.

IE3D simulation results are presented for RMSA with single U-shaped slot. The effect of varying slot dimensions on the bandwidth is also studied. It is found that notch resonant frequency is governed by the physical length of the U-slot.

Simulation results are also presented for RMSA with double U-slots. It attained an antenna impedance bandwidth of 40%. Orthogonal mode excitation gives rise to switch of polarization within the bandwidth.

It is found that a TMSA with an U-slot shows wideband characteristics. Unlike RMSA with a U-slot, it does not show switch of polarization.

A U-slot patch antenna, which can function properly both in the WLL and GSM frequency bands, is designed, fabricated and tested.

## List of symbols

$\epsilon_r$	relative dielectric constant
$\lambda_0$	free space wavelength
$\phi$	azimuth angle
$\theta$	elevation angle
$\eta$	radiation efficiency
$c$	free space velocity of light
$D$	directivity of the antenna
$f_r$	resonant frequency
$G$	gain of the antenna
$h$	height of the antenna
$L$	length of the antenna
$P_0$	power accepted by the antenna
$P_r$	radiated power from the antenna
$R_{rad}$	radiation resistance of the antenna
$\tan\delta$	loss tangent of the substrate
$U$	radiation intensity
$W$	width of the patch

## Acronym

GSM	Geosynchronous mobile
MSA	Microstrip antenna
RMSA	Rectangular microstrip antenna
TMSA	Triangular microstrip antenna
VSWR	Voltage standing wave ratio
WLL	Wireless local loop

# Table of Contents

---

Contents	Page No.	
<b>Chapter 1</b>		
<b>Introduction</b>		
1.1	Bandwidth of an Antenna	1
1.2	Microstrip antenna element design parameters	1
	1.2.1 Feed point to the patch antenna	2
1.3	Radiation pattern	2
1.4	Antenna efficiency and gain	2
1.5	Literature survey	3
	1.5.1 Bandwidth enhancement of a RMSA by integrative loading	4
	1.5.2 Notched RMSA	4
	1.5.3 Two-layer electromagnetically coupled RMSA	4
	1.5.4 Aperture fed stacked configuration	4
	1.5.5 Motivation for the project	4
1.6	Organization of the project report	5
<b>Chapter 2</b>		
<b>Simulation studies of the effect of varying slot dimensions on the U-slot RMSA</b>		
2.1	Introduction	6
2.2	Antenna geometry	6
2.3	Simulation results	7
	(a) prototype single U-slot RMSA	7
	(b) RMSA without U-slot	12
	(c) Effect of varying slot dimensions	13
<b>Chapter 3</b>		
<b>A RMSA with double U-shaped slot and multiple polarization</b>		
3.1	Introduction	19
3.2	Double U-slot RMSA	19
3.3	Simulation results of double U-slot RMSA	20

## **Chapter 4**

### **TMSA with a U-shaped slot**

4.1	Introduction	25
4.2	U-slot TMSA	26
4.3	Simulation results of U-slot TMSA	27

## **Chapter 5**

### **Experimental and simulation studies of WLL and GSM frequency band U-slot RMSA**

5.1	Introduction	31
5.2	Experimental and simulation studies of WLL and GSM frequency band U-slot RMSA	32

## **Chapter 6**

### **Conclusion**

6.1	Conclusion	40
6.2	Further investigations	41

<b>References</b>	42
-------------------	----

<b>Appendix</b>	44
-----------------	----



## List of Figures

Figure No.	Description	Page No.
1.1	Rectangular microstrip antenna element	1
1.2	Typical E- and H-plane patterns of a typical RMSA	2
2.1	Geometry of U-slot RMSA	6
2.2	Input impedance locus of the prototype U-slot RMSA	8
2.3	VSWR vs frequency for the prototype U-slot RMSA	8
2.4	Radiation patterns at 4.1 GHz	9
2.5	Radiation patterns at 4.7 GHz	10
2.6	Radiation patterns at 5.3 GHz	11
2.7	Broadside gain against frequency	12
2.8	Input impedance loci of RMSA without U-slot	12
2.9	VSWR vs frequency of RMSA without U-slot	13
2.10	Input impedance locus and VSWR vs frequency for Horz_long U-slot RMSA	14
2.11	Input impedance locus and VSWR vs frequency for Vert_long U-slot RMSA	15
2.12	Impedance locus and VSWR vs frequency for Vert_short U-slot RMSA	16
2.13	Impedance locus and VSWR vs frequency for Horz-short U-slot RMSA	17
2.14	Impedance locus and VSWR vs frequency for Slot_width U-slot RMSA	18
3.1	Geometry of double U-slot RMSA	19
3.2	Impedance loci of double U-slot RMSA	20
3.3	VSWR vs frequency for double U-slot RMSA	21
3.4	Broadside gain vs frequency for double U-slot RMSA	21
3.5	Radiation patterns at 1.34 GHz	22
3.6	Radiation patterns at 1.64 GHz	23
3.7	Radiation pattern at 1.94 GHz	24
4.1	Geometry of a U-slotted TMSA	25
4.2	Impedance locus of a U-slot TMSA	26
	VSWR vs frequency for U-slot TMSA	27
4.3	Broadside gain vs frequency for U-slot TMSA	27
4.4	Radiation patterns at 1.55 GHz	28
4.5	Radiation patterns at 1.70 GHz	29
4.6	Radiation patterns at 1.85 GHz	30

5.1	Side view of the WLL and GSM band antenna	31
5.2	Photograph of the WLL and GSM band U-slot RMSA	32
5.3	Impedance locus of WLL and GSM band U-slot RMSA	33
5.4	VSWR vs frequency for WLL and GSM band U-slot RMSA (Antenna B)	33
5.5	Radiation pattern for antenna B at 0.75 GHz	34
5.6	Radiation patterns for antenna B at 0.85 GHz	35
5.7	Radiation patterns for antenna B at 0.95 GHz	36
5.8	Radiation patterns for Antenna A at 0.95 GHz	37
5.9	Broadside gain vs frequency for Antenna A and B	38
5.10	Measured impedance loci and return loss of antenna A	39
A.1	Coaxial cable	44

## List of Tables

Table No.	Description	Page No.
2.1	Dimensions of prototype U-slot RMSA in mm.	7
2.2	Variations on the slot dimensions to study its effects on antenna performance	7
4.1	Dimensions of the U-slot TMSA in mm.	25
5.1	Dimensions of the WLL and GSM U-slot RMSA	31

## Chapter 1

### Introduction

#### 1.1 Bandwidth of an Antenna

All antennas are limited in the range of frequency over which they will operate satisfactorily. This range is called the bandwidth of the antenna. There are many factors involved in deciding the antenna bandwidth. For single MSA elements, the impedance bandwidth is generally the limiting factor. The impedance variation with frequency of the antenna element results in a limitation of the frequency range over which the element can be matched to its feed line. Impedance bandwidth is usually specified in terms of a return loss or maximum SWR (typically less than 2.0) [1,2].

#### 1.2 Microstrip antenna element design parameters

The most commonly used microstrip element consists of a rectangular element (Fig. 1-1). The element is fed with a coaxial feed. The length  $L$  is the most critical dimension and is slightly less than a half wavelength in the dielectric substrate material.

$$f_r = [c / (2L\sqrt{\epsilon_r})] \quad (1.1)$$

where  $L$  = length of the patch

$\epsilon_r$  = relative dielectric constant of the substrate

$c$  = free space velocity of light

$f_r$  = resonant frequency of the patch

The width of the antenna must be less than a wavelength in the dielectric substrate material so that higher modes will not be excited [3].

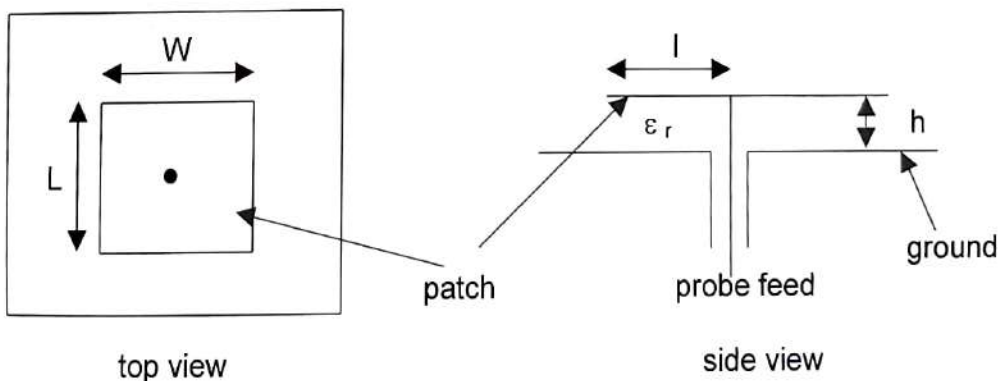


**Fig. 1.1 Rectangular microstrip antenna element**

### 1.2.1 Feed point to the patch antenna

The feed point is very important for a good match, which increases the bandwidth. A patch with an inset feed point has a resonant resistance given by

$$R_{rad} = R_{rad}^e \cos^2(\pi/L) \tag{1.2}$$

where  $R_{rad}^e$  is the radiation resistance of an antenna fed at the edge [2].

### 1.3 Radiation pattern

If an antenna is imagined to be located at the center of a spherical coordinate system, its radiation pattern is determined by measuring the electric field intensity over the surface of a sphere at some fixed distance. Although, the total pattern of an antenna is three dimensional, the pattern is usually represented in terms of two-dimensional patterns in two planes that form 90 degrees angle with each other.

The  $\phi = 0^\circ$  and  $\phi = 90^\circ$  plane patterns are the principal-plane patterns of a patch antenna. The principal plane patterns a typical MSA is shown in Fig. 1.2.

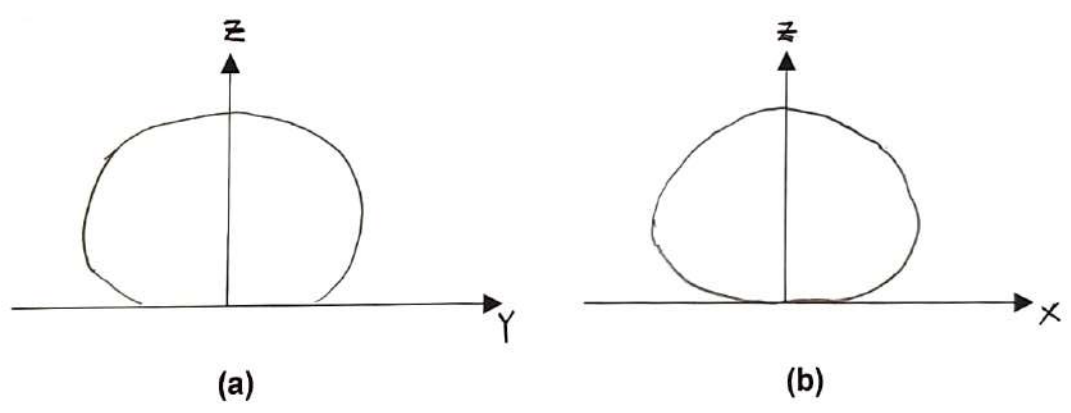


Fig. 1.2 Typical E- and H- plane patterns of a typical RMSA

- a - E-plane
- b - H-plane

It is also fairly common to express the relative field strength or power density in decibels. This coordinate of pattern is given as  $20 \log (E/ E_{max})$  or  $10 \log (P/P_{max})$  [1,4,21].

## 1.4 Antenna efficiency and gain

Consider an antenna which is located at the origin of a spherical coordinate system. Suppose that we are making observations on spherical shell having a very large radius  $r$ .

Assume that the antenna is transmitting, and let

- $P_0$  = power accepted by the antenna, watts
- $P_r$  = power radiated by the antenna, watts
- $\eta$  = radiation efficiency, unitless

The above quantities are related as follows:

$$\eta = P_r/P_0 \quad (1.3)$$

Let  $U(\theta, \phi)$  = radiation intensity, watts/ steradians

The total radiated power from the antenna is

$$P_r = \int \int U(\theta, \phi) \sin\theta \delta\theta \delta\phi \quad (1.4)$$

and average radiation intensity is

$$U_{\text{avg}} = P_r / 4\pi \quad (1.5)$$

Let

- $D(\theta, \phi)$  = directivity, unitless

Directivity is the measure of the ability of antenna to concentrate radiated power in a particular direction, and it is related to the radiation intensity as follows:

$$D(\theta, \phi) = U(\theta, \phi) / U_{\text{avg}} = U(\theta, \phi) / (P_r / 4\pi) \quad (1.6)$$

Let

- $G(\theta, \phi)$  = gain, unitless

The gain of an antenna is related to directivity and power radiation intensity as follows:

$$G(\theta, \phi) = \eta D(\theta, \phi) = [\eta U(\theta, \phi) / (P_r / 4\pi)] = [U(\theta, \phi) / (P_0 / 4\pi)] \quad (1.7)$$

Thus the gain is the measure of the ability to concentrate in a particular direction the power accepted by the antenna [3].

## 1.5 Literature survey

Some of the bandwidth enhancement techniques are summarized below:

### 1.5.1 Bandwidth enhancement of a RMSA by integrated reactive loading

The resonant frequency of a RMSA can be changed by using reactive loading. It is possible to design an antenna with more than one resonant frequency. By choosing the resonant frequency close to each other, a broadband element with a bandwidth of almost three times larger than that of a single resonant patch can be achieved [5].

### 1.5.2 Notched RMSA

The main idea in this is to design a reactive load by cutting a notch (or notches). A properly designed notch patch can exhibit an impedance bandwidth of 38% [6,7].

### 1.5.3 Two-layer electromagnetically coupled RMSA

It consist of a driven patch in the bottom and a parasitic patch on the top. The two layers are separated by an air region. Bandwidth of 13% has been reported [8].

### 1.5.4 Aperture fed stacked configuration

In the aperture coupled antenna, the field is coupled from the microstrip feedline placed on the other side of the ground plane to the radiating patch through an electrically small aperture in the ground plane. Bandwidth of 40% at 4.64 GHz has been reported [9].

### 1.5.5 Motivation for the project

MSAs are known to have a narrow bandwidth of the order of  $\sim 2\text{-}5\%$  ( $\text{SWR} \leq 2$ ). By increasing the thickness of the substrate, a bandwidth of maximum 10% can be achieved [10,27]. But, it gives rise to problem of surface wave excitation, increased probe reactance, etc. Parasitic patches, either in another layer (stacked geometry) or in the same layer (coplanar geometry), have the disadvantage of increasing the antenna volume.

Recently, Lee *et al* [11] designed a broadband antenna (of bandwidth greater than 30%) by simply cutting a U-shaped slot without increasing the antenna volume. MSA with a U-slot is compact and maintains its thin profile. This method gives much broader bandwidth than most of the conventional techniques. There is a need to study this particular antenna in detail.

## **1.6 Organization of the project report**

An extensive literature survey on the conventional bandwidth enhancement techniques shows that U-slotted antennas are compact, broadband and maintains thin profile characteristics as described in chapter 1.

An extensive simulation studies of the effect of changing slot dimensions on the bandwidth of a coaxially fed RMSA with a single U-slot is presented in chapter 2. It is of interest to see how the antenna would perform if there were no U-slot. This is also discussed in this chapter.

Chapter 3 discusses about an RMSA with double U-slot which has a better bandwidth than a RMSA with a single U-slot. The switch of polarization within the bandwidth owing to excitation of orthogonal modes is also brought forward.

In Chapter 4, a TMSA with an U-shaped slot is studied. This antenna also shows broadband characteristics.

Chapter 5 presents experimental and simulation studies of a RMSA which can work both in WLL (824-890 MHz) and GSM (890-960 MHz) frequency bands.

Chapter 6 concludes the thesis with conclusion and topics which can be further investigated.



## Chapter 2

### Simulation studies of the effect of varying slot dimensions on the U-slot RMSA

#### 2.1 Introduction

An extensive simulation results of the effect of slot dimensions on the impedance bandwidth, co-polarization and cross-polarization pattern characteristics and gain is presented and compared with the case if there were no U-slot on the patch. IE3D 6.03 simulator is used for all simulation works [12,13,17].

#### 2.2 Antenna geometry

The geometry of the antenna is as shown in Fig. 2.1.

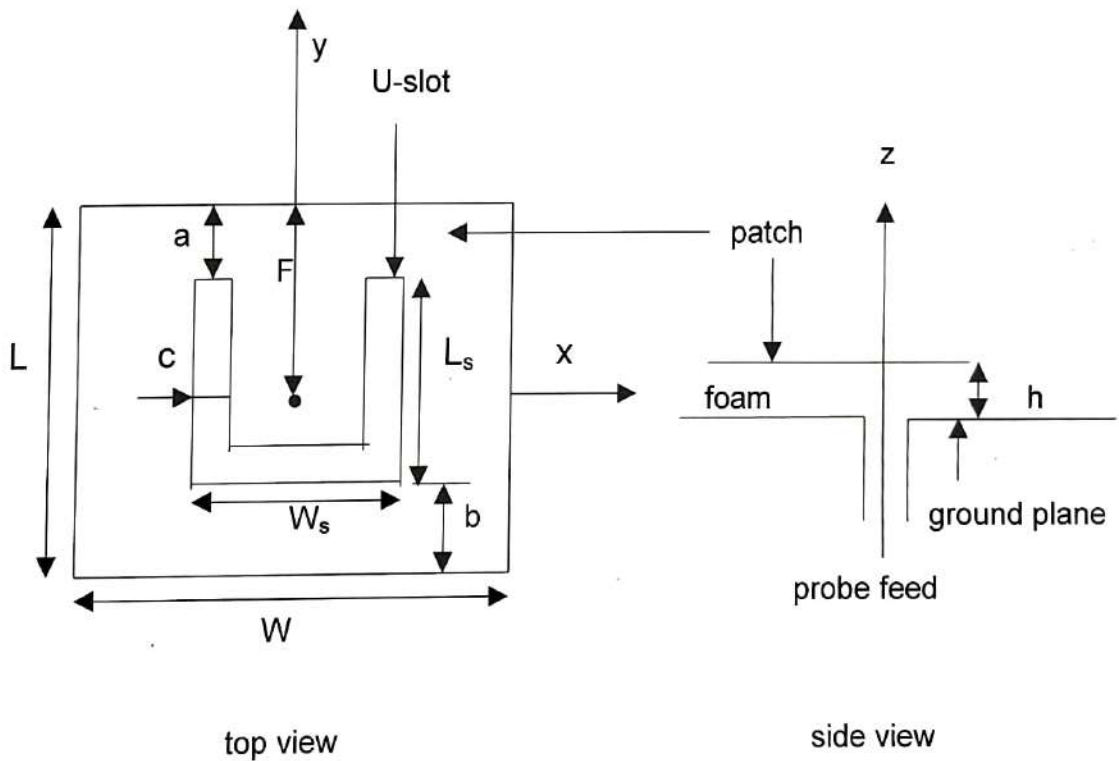


Fig. 2.1 Geometry of U-slot RMSA

The prototype U-slot RMSA has dimensions as given in Table 2.1.

Table 2.1 Dimensions of prototype U-slot RMSA in mm.

W	L	F	$W_s$	$L_s$	a	b	c	h
35.5	26.0	15.0	12.0	19.5	2.2	4.3	2.1	5.0

The dielectric medium between the patch and ground plane is foam substrate ( $\epsilon_r = 1.01$ ). The patch is fed by a 50  $\Omega$  coaxial probe of inner diameter 1.2 mm. To study the effect of varying one of the slot dimensions on the antenna performance, the following modifications are done on the prototype antenna, keeping the other parameters fixed.

Table 2.2 Variations on the slot dimensions to study its effects on antenna performance.

Sl. No.	U-slot RMSA	$W_s$ (mm)	$L_s$ (mm)	c (mm)	Total slot length (mm)
1	Horz_long	12.0+4.0	19.5	2.1	46.9+4.0
2	Vert_long	12.0	19.5+1.0	2.1	46.9+2.0
3	Vert_short	12.0	19.5-1.0	2.1	46.9-2.0
4	Horz_short	12.0-4.0	19.5	2.1	46.9-4
5	Slot_width	12.0	19.5	2.1+0.9	46.9-1.8

## 2.3 Simulation results

### a) Prototype antenna

The input impedance locus of the prototype U-slot RMSA is shown in Fig. 2.2. VSWR is plotted against frequency for the same antenna in Fig. 2.3. The antenna is linearly polarized, with electric field parallel to the y-axis and magnetic field parallel to the x-axis.

Figs. 2.4-2.6 show the radiation patterns in the  $\phi = 0^\circ$  plane (H-plane) and  $\phi = 90^\circ$  plane (E-plane) at the three different frequencies. In the H-plane, the cross-polarization remains less than  $-20$  dB for all frequencies. In the E-plane ( $\phi = 90^\circ$  plane), the cross-polarization is so small that it does not show up.

The broadside gain is plotted against frequency in Fig. 2.7. The gain of the antenna is greater than 8 dB from 3.9 GHz to 5.25 GHz. The half-power beamwidths in the E-plane and H-plane are about  $60^\circ$  at all frequencies.

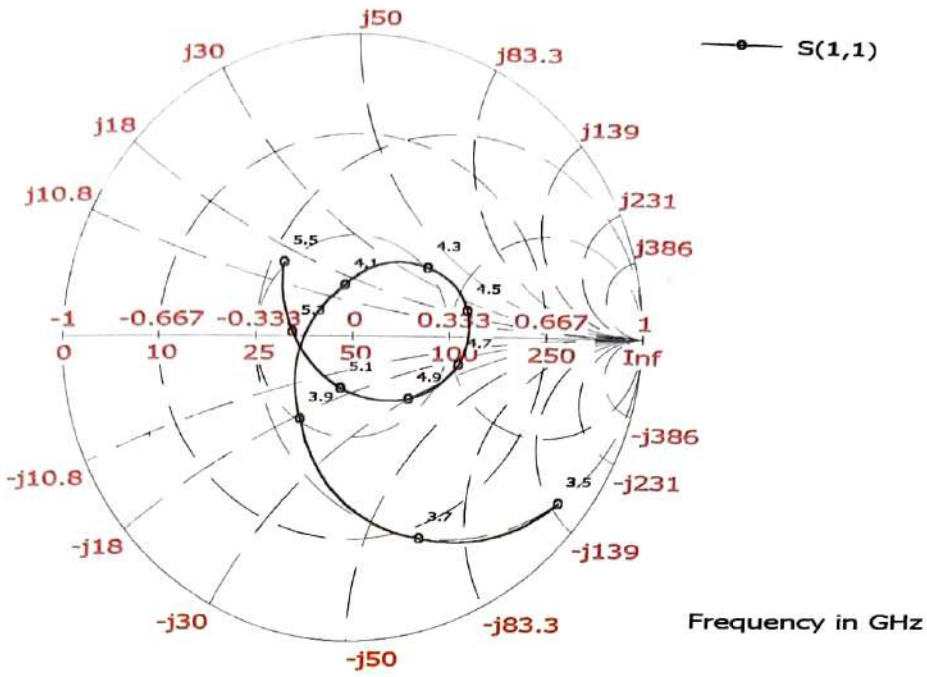


Fig. 2.2 Input impedance locus of the prototype U-slot RMSA

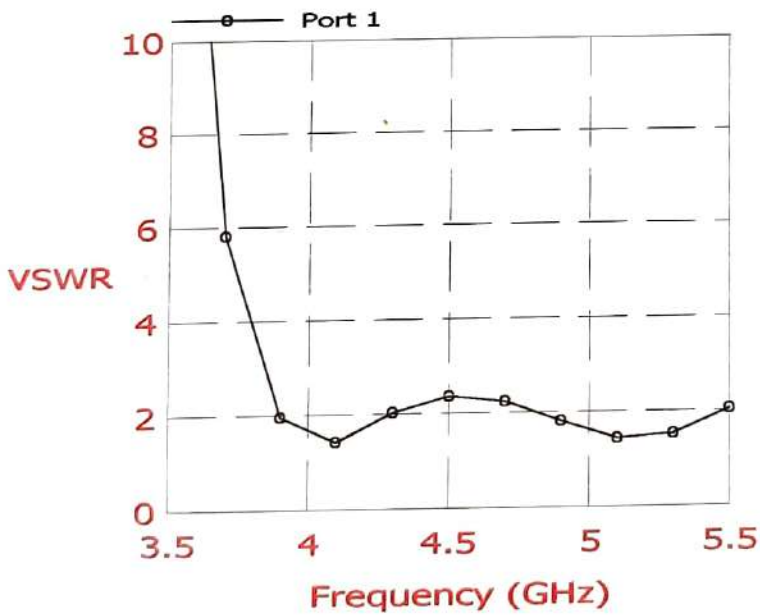
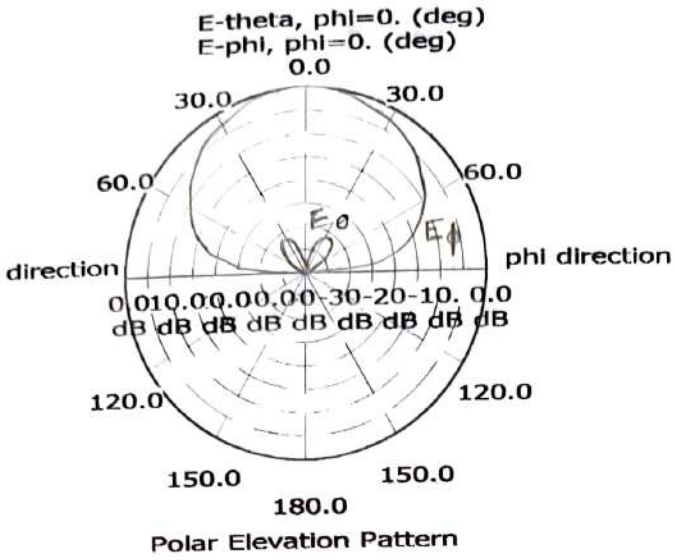
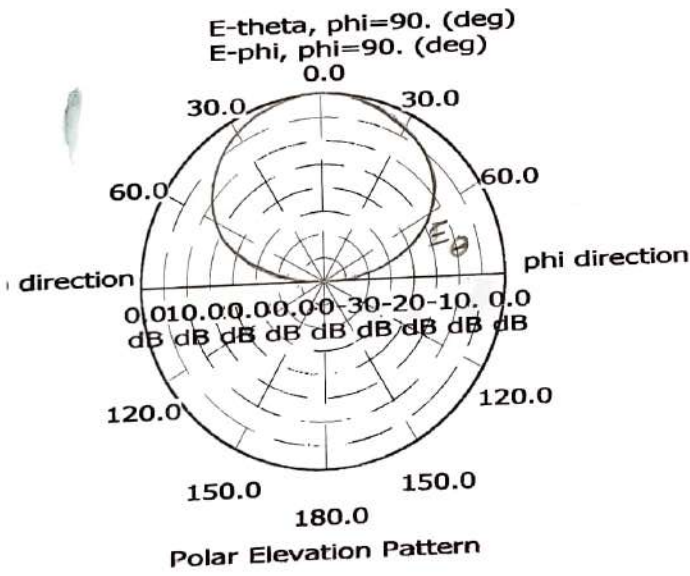


Fig. 2.3 VSWR vs frequency for the prototype U-slot RMSA



(a)  $\phi = 0^\circ$

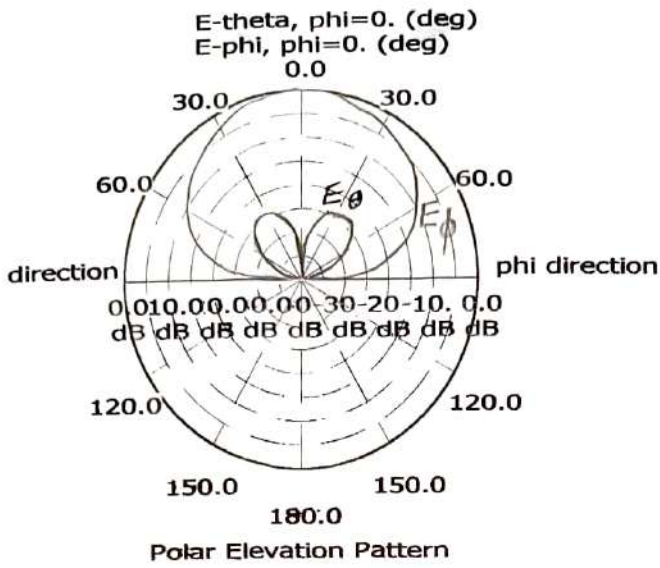


(b)  $\phi = 90^\circ$

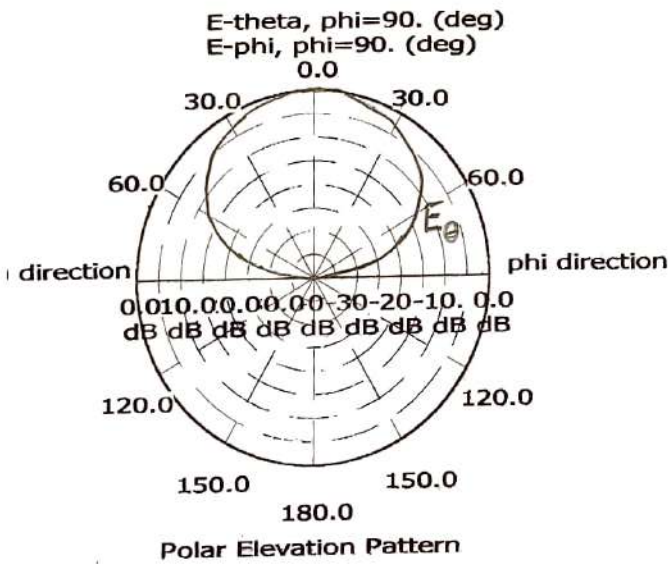
Fig. 2.4 Radiation patterns at 4.1 GHz

a - H-plane

b - E-plane



(a)  $\phi = 0^\circ$



(b)  $\phi = 90^\circ$

Fig. 2.5 Radiation patterns at 4.7 GHz

- a- H-plane
- b- E-plane

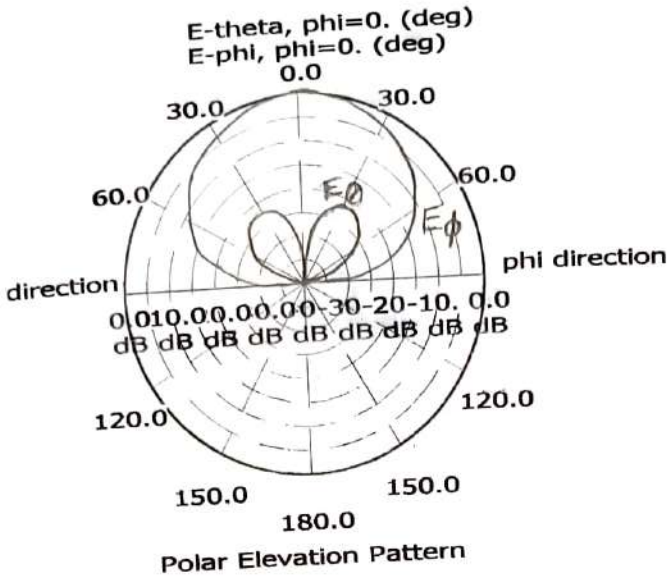
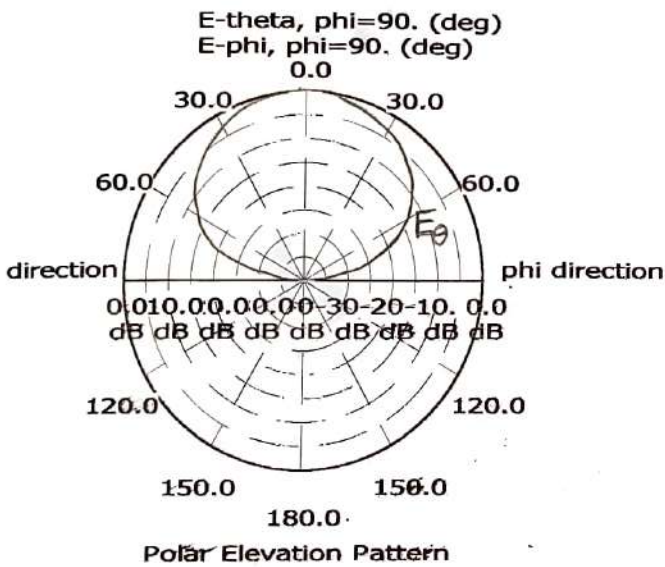
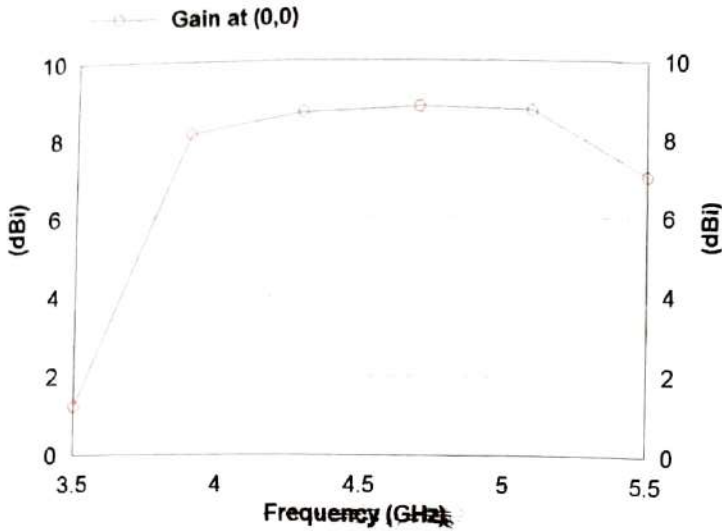
(a)  $\phi = 0^\circ$ (b)  $\phi = 90^\circ$ 

Fig. 2.6 Radiation patterns at 5.3 GHz

- a- H-plane
- b- E-plane

### Gain Vs. Frequency



**Fig. 2.7 Broadside gain against frequency**

b) To see how the RMSA would perform if there were no U-slot, simulation results are presented for RMSA of same dimensions without U-slot. The input impedance locus is shown in Fig. 2.8 for two feed positions, shows that the input impedance has very large inductive. VSWR is plotted against frequency in Fig. 2.8 which shows that it is not possible to obtain a VSWR less than 2 for any feed position.

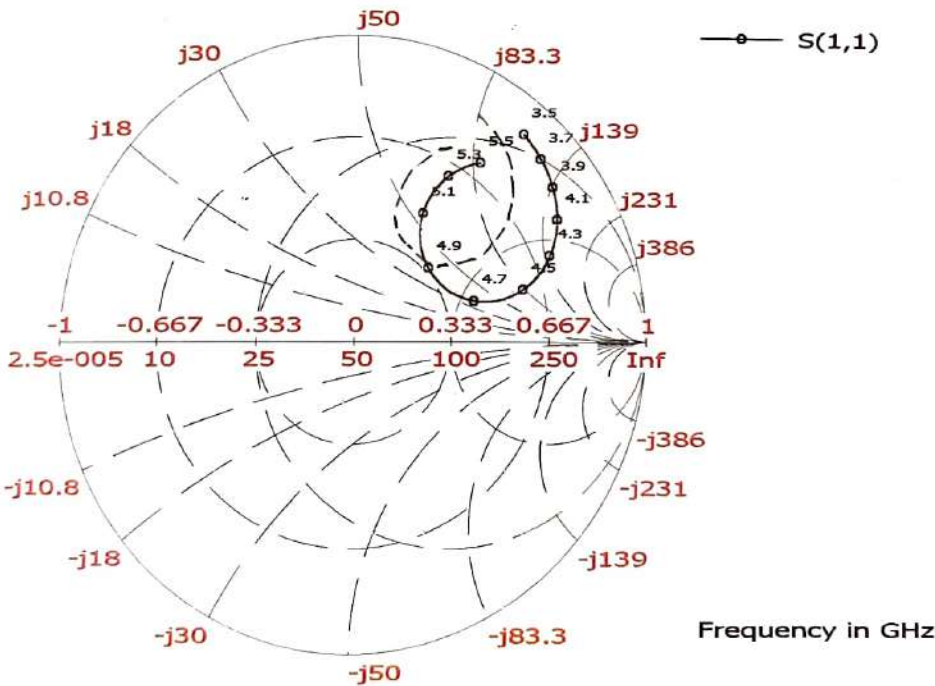


**Fig. 2.8 Input impedance loci of RMSA without U-slot (—) edge fed, (- - -) fed 2 mm. from the edge toward the center.**

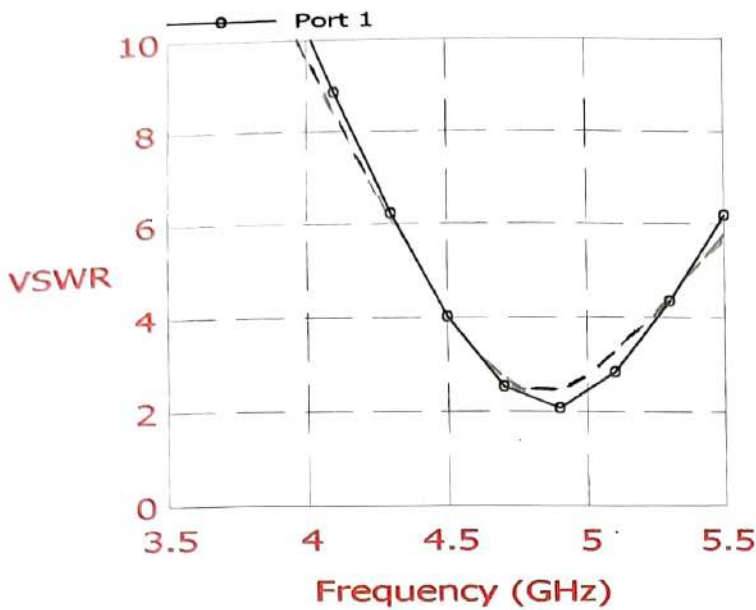


**Fig. 2.9 VSWR vs frequency of RMSA without U-slot (—) edge fed (- - -) fed 2 mm. from the edge towards the center**

### c) Effect of varying slot dimensions

For different RMSAs which are formed by changing the slot dimensions as indicated in Table 2.2, the input impedance locus and VSWR is plotted against frequency in Figs. 2.10 to 2.14. By changing the length of the horizontal or vertical slots or slot width, we basically changes the total slot length as shown on table 2.2. As the total length of the slot is decreased in the serial order as shown on the table, we can infer the following:

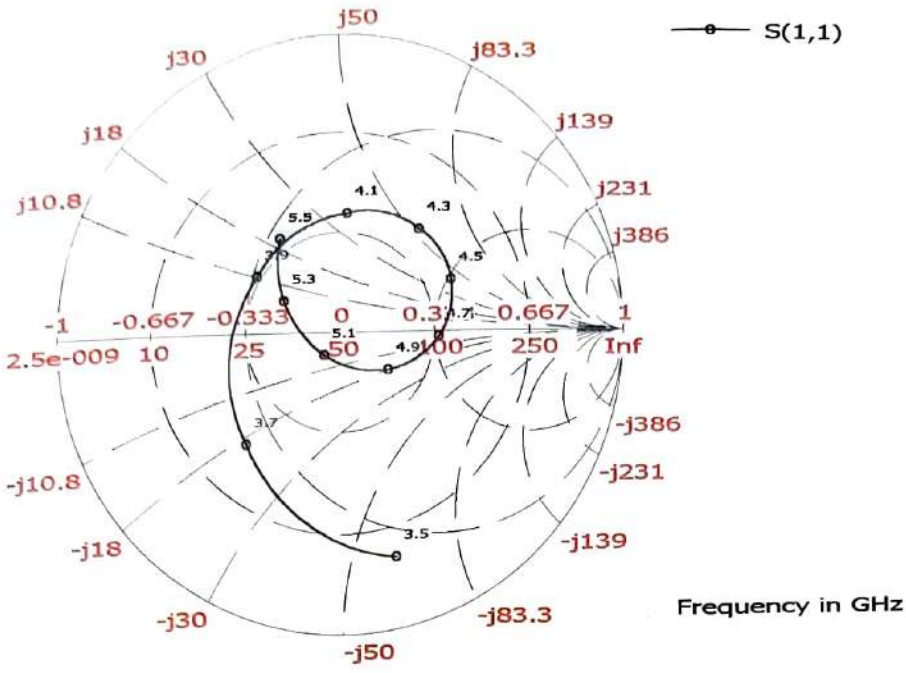
Firstly, the impedance locus shifts downward on the smith chart thereby showing an increased capacitive component in the input impedance of the antenna.

Secondly, the notch resonant frequency is increased. Hence, the notch resonant frequency is governed by the total U-slot length.

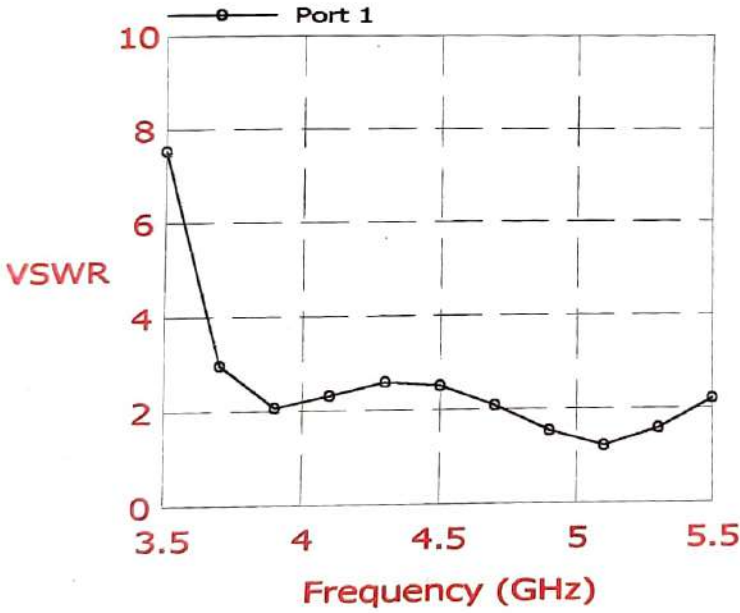
Thirdly, changing slot width has effect far more pronounced on the input impedance and notch resonant frequency than all other cases. Even if increasing slot width increases the total slot length, its effect is more than just this as shown in fig. 2.14.

The broadside gain vs frequency, E- and H- planes radiation patterns are very similar to that of the prototype U-slot RMSA. They are not shown for simplicity.



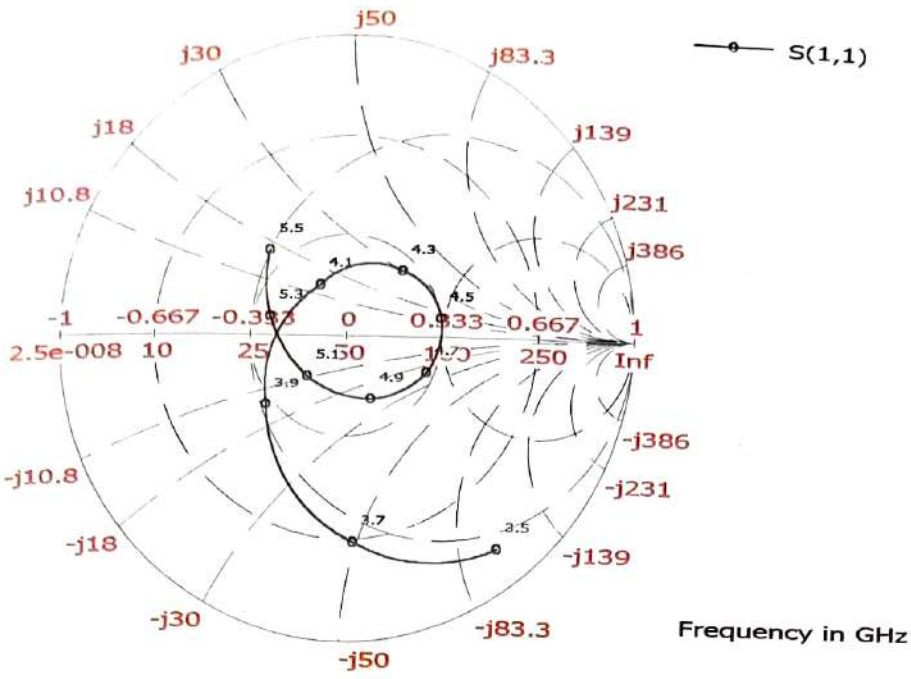


(a)

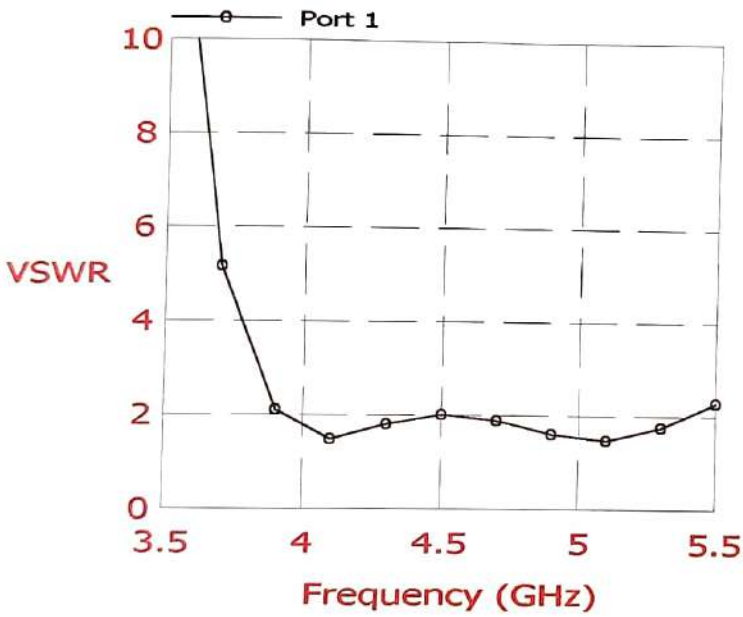


(b)

Fig. 2.10 (a) Input impedance locus and (b) VSWR vs frequency for Horz\_long U-slot RMSA

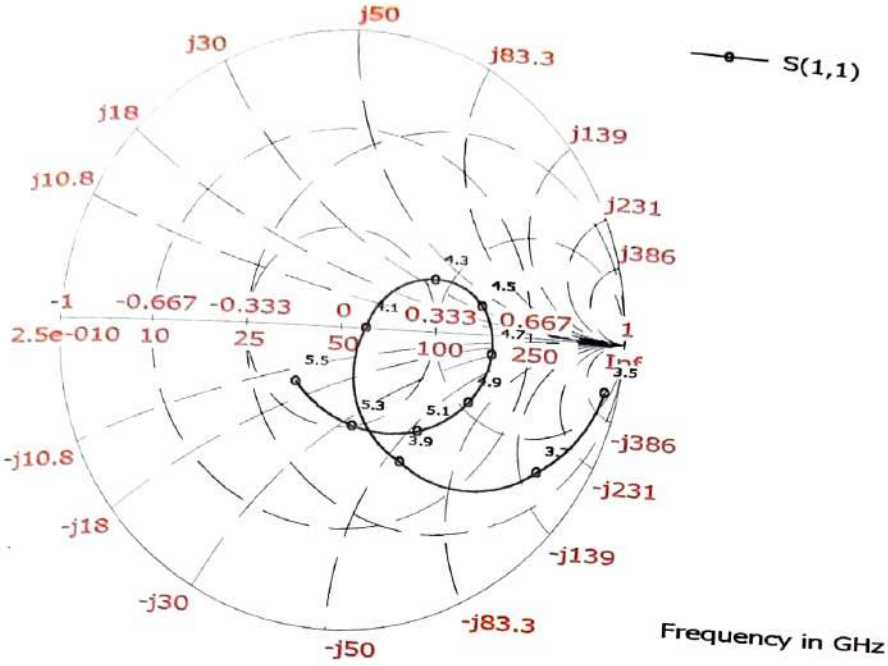


(a)

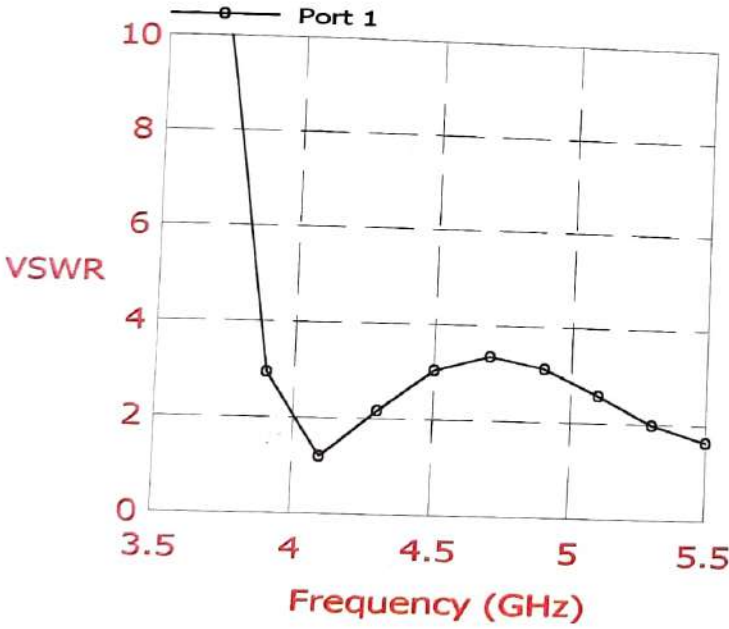


(b)

Fig. 2.11 (a) Input impedance locus and (b) VSWR vs frequency for Vert\_long U-slot RMSA

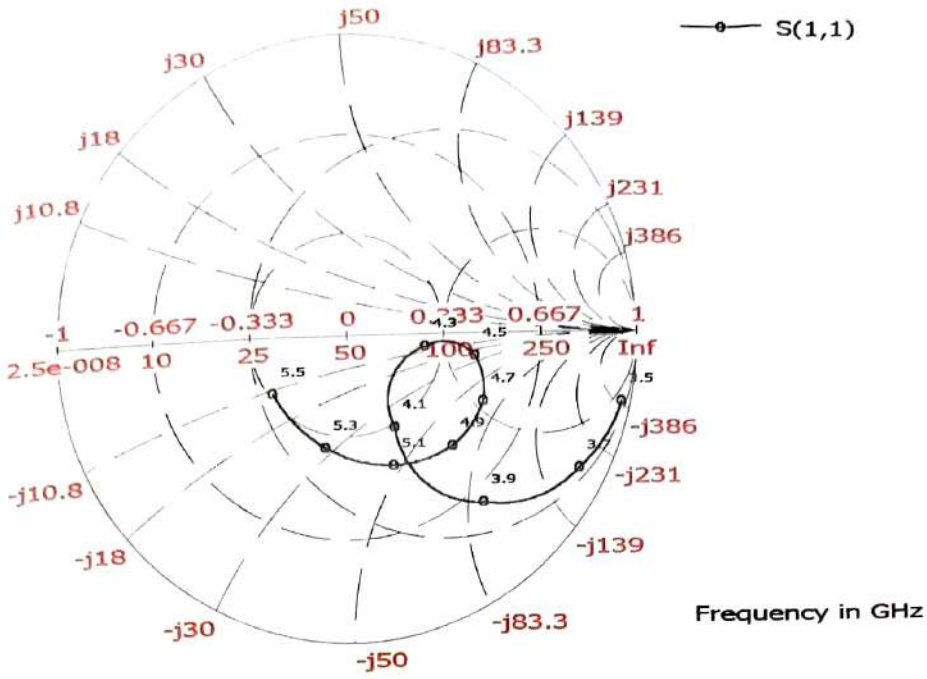


(a)

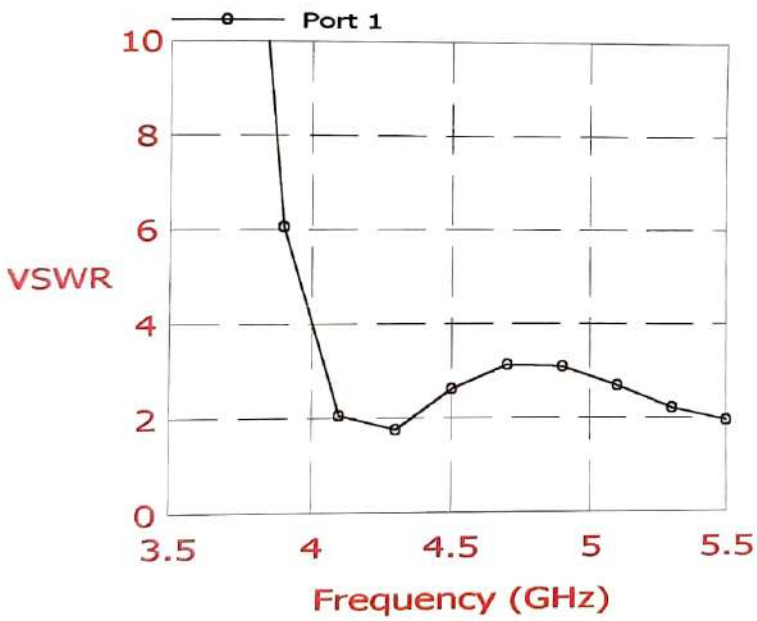


(b)

Fig. 2.12 (a) Input impedance locus and (b) VSWR vs frequency for Vert\_short U-slot RMSA



(a)



(b)

Fig. 2.13 (a) Input impedance locus and (b) VSWR vs frequency for Horz\_short U-slot RMSA

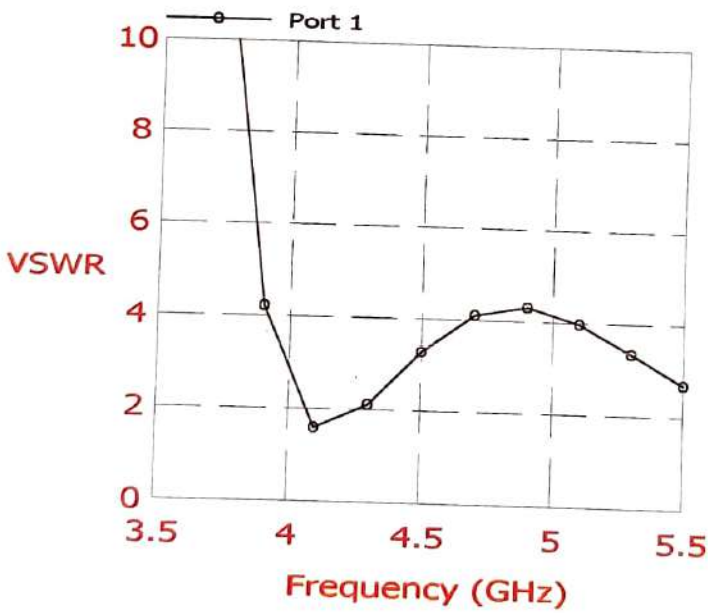
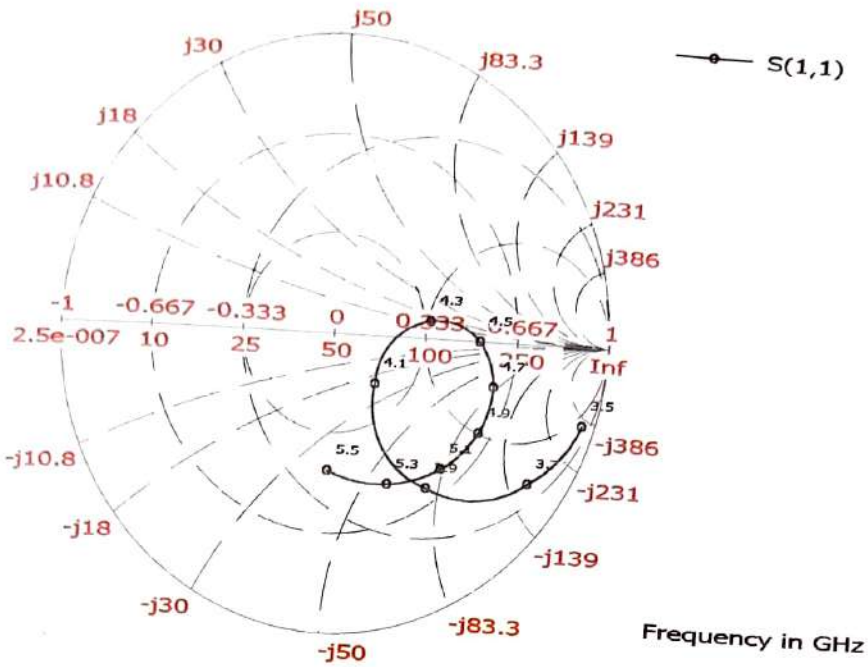


Fig. 2.14 (a) Input impedance locus and (b) VSWR vs frequency for Slot\_width U-slot RMSA

## Chapter 3

# A RMSA with double U-shaped slot and multiple polarization

## 3.1 Introduction

Simulation results on a RMSA with double U-shaped slot are presented. This antenna has 40% impedance bandwidth. Radiation characteristics over the bandwidth show that there is switch in polarization due to excitation of orthogonal modes [14,15].

## 3.2 Double U-slot RMSA

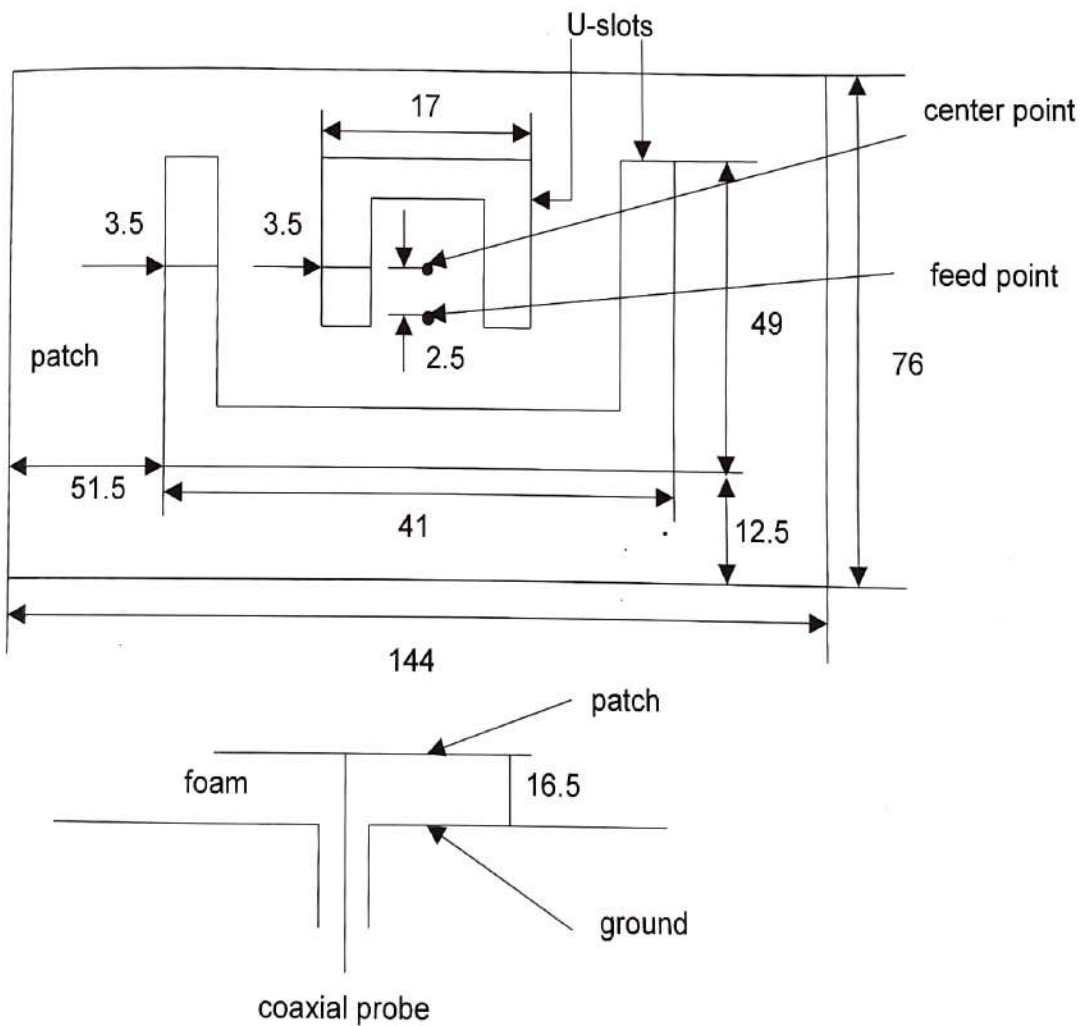


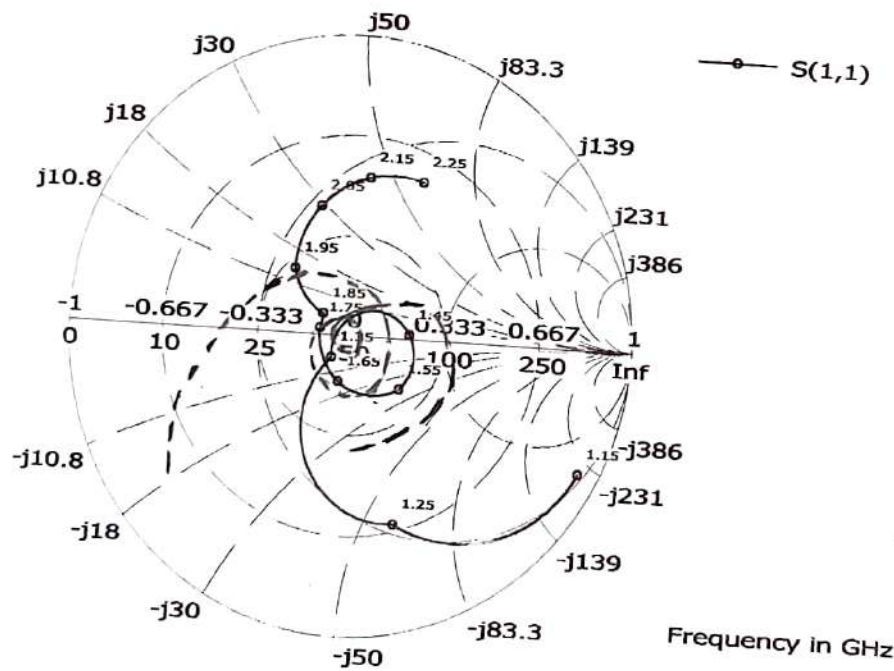
Fig. 3.1 Geometry of double U-slot RMSA

The geometry of the antenna is shown in Fig. 3.1. All dimensions are in mm. The height of the foam ( $\epsilon_r = 1.01$ ) is 16.5mm. The patch is fed by a  $50\Omega$  coaxial probe of inner diameter 9mm..

### 3.3 Simulation results:

The input impedance loci is shown in Fig. 3.2. It shows an additional loop due to the second U-slot. The VSWR is plotted against frequency is given in Fig. 3.3. The impedance bandwidth (SWR<2) is 40%. The broadside gain is plotted against frequency in Fig. 3.4. It shows a broad gain of 8 db or more from 1.3 to 1.7 GHz.

The E-plane and H-plane radiation patterns are shown at three different frequencies are shown in Figs. 3.5-3.7. In the reported result, radiation patterns was measured only at 1.59 GHz [14]. IE3D simulation results show that cross-polarization increases at higher frequencies and polarization switch is seen at 1.94GHz frequency. It is due to excitation of orthogonal modes. In the E-plane, the cross-polarization is so low that it does not show up. The half-power beamwidth in the E-plane and H-plane is about  $60^\circ$  for 1.34GHz and 1.64GHz.



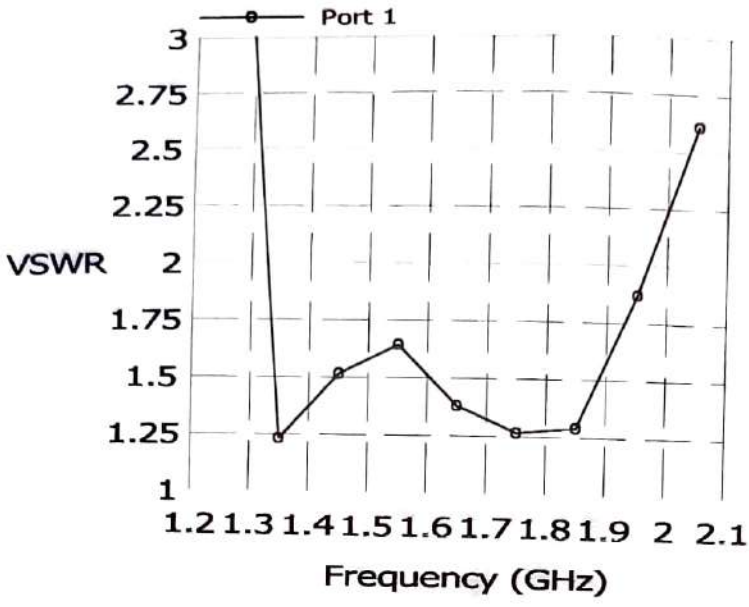


Fig. 3.3 VSWR vs frequency for double U-slot RMSA

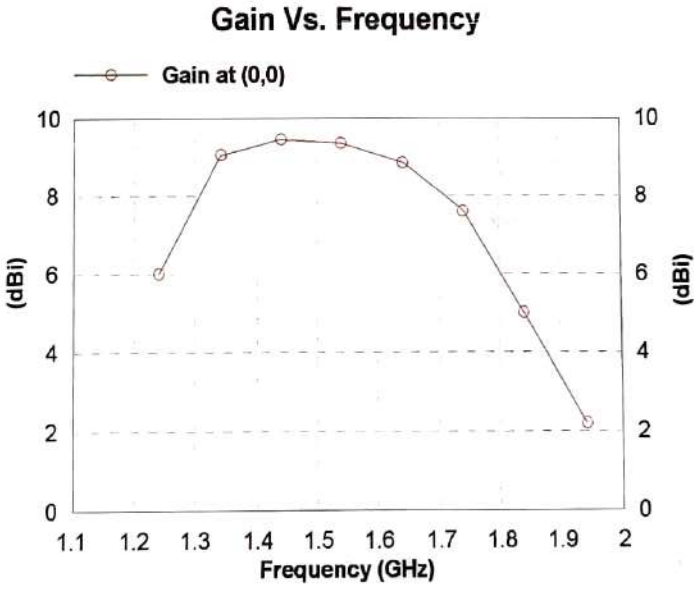


Fig. 3.4 Broadside gain against frequency for double U-slot RMSA



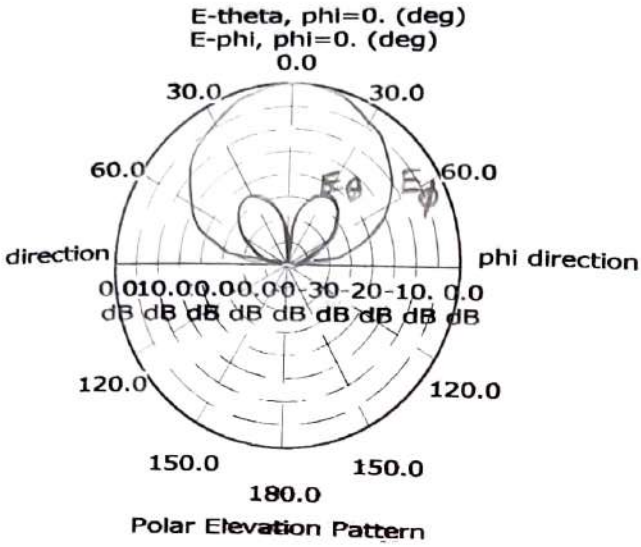
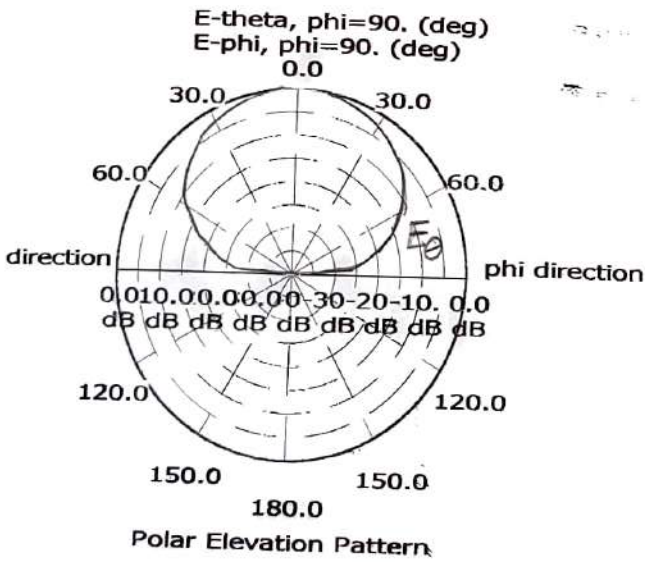
(a)  $\phi = 0^\circ$ (b)  $\phi = 90^\circ$ 

Fig. 3.5 (a) Radiation patterns at 1.34 GHz (a)- H-plane (b)- E-plane

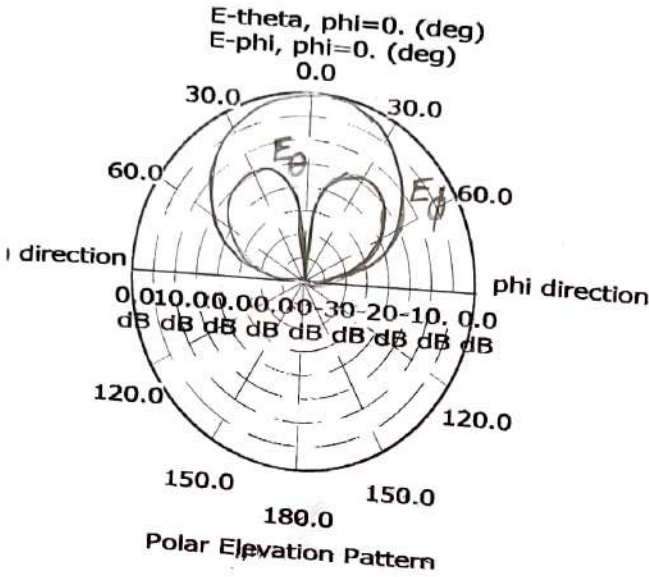
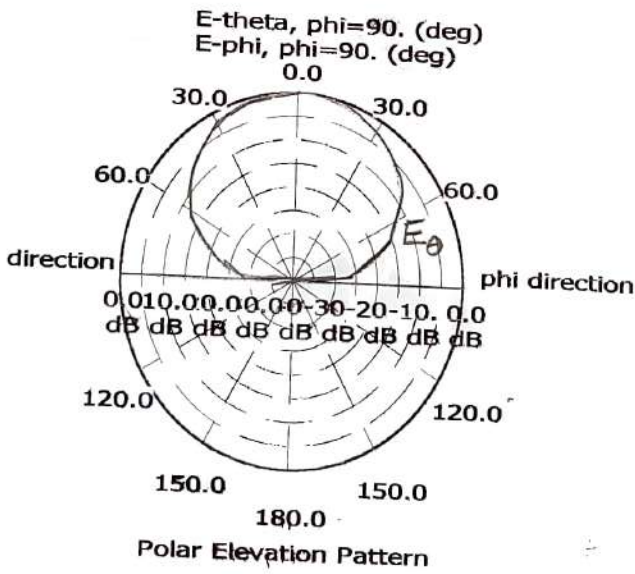
(a)  $\phi = 0^\circ$ (b)  $\phi = 90^\circ$ 

Fig. 3.6 Radiation patterns at 1.64 GHz (a)- H-plane (b)- E-plane

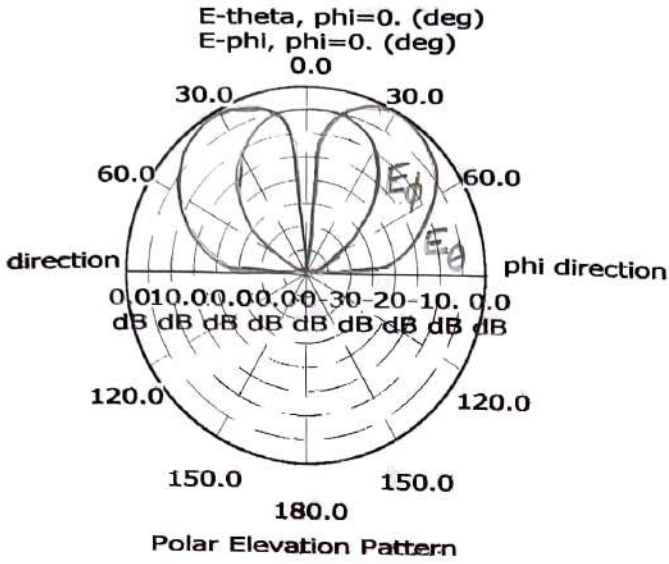
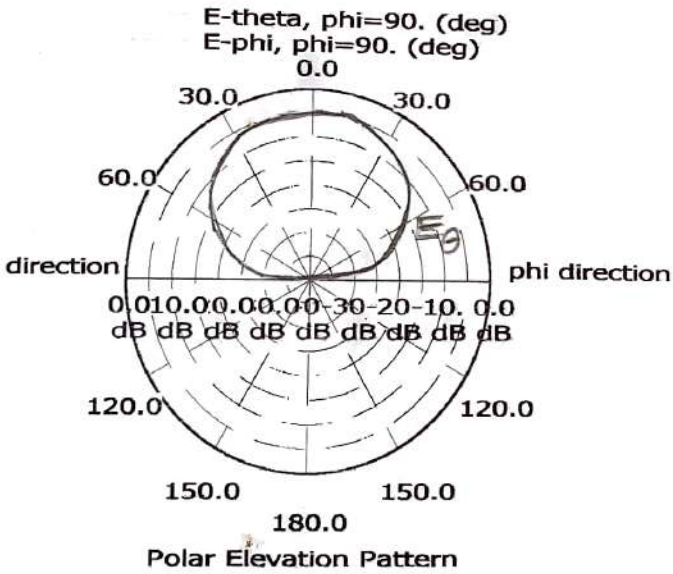
(a)  $\phi = 0^\circ$ (b)  $\phi = 90^\circ$ 

Fig.3.7 Radiation patterns at 1.94 GHz (a)- H-plane (b)- E-plane

## Chapter 4

### TMSA with a U-shaped slot

#### 4.1 Introduction

Bandwidth enhancement by cutting a U-shaped slot is also possible for a TMSA. It has the advantage of being physically smaller than a corresponding RMSA. Simulation results for an equilateral TMSA is presented which shows broadband characteristics [16].

#### 4.2 U-slot TMSA

Fig. 4.1 shows the geometry of TMSA with a U-shaped slot. The dimensions of the antenna are as shown in table 4.1.

Table 4.1 Dimensions of the equilateral TMSA in mm.

h	S	$d_1$	$d_2$	$\alpha$	$d_p$	$l_1$	$l_2$	$w_1$	$w_2$
14.3	3.2	91.0	91.0	$60^\circ$	26.2	46.2	24	6	2.5

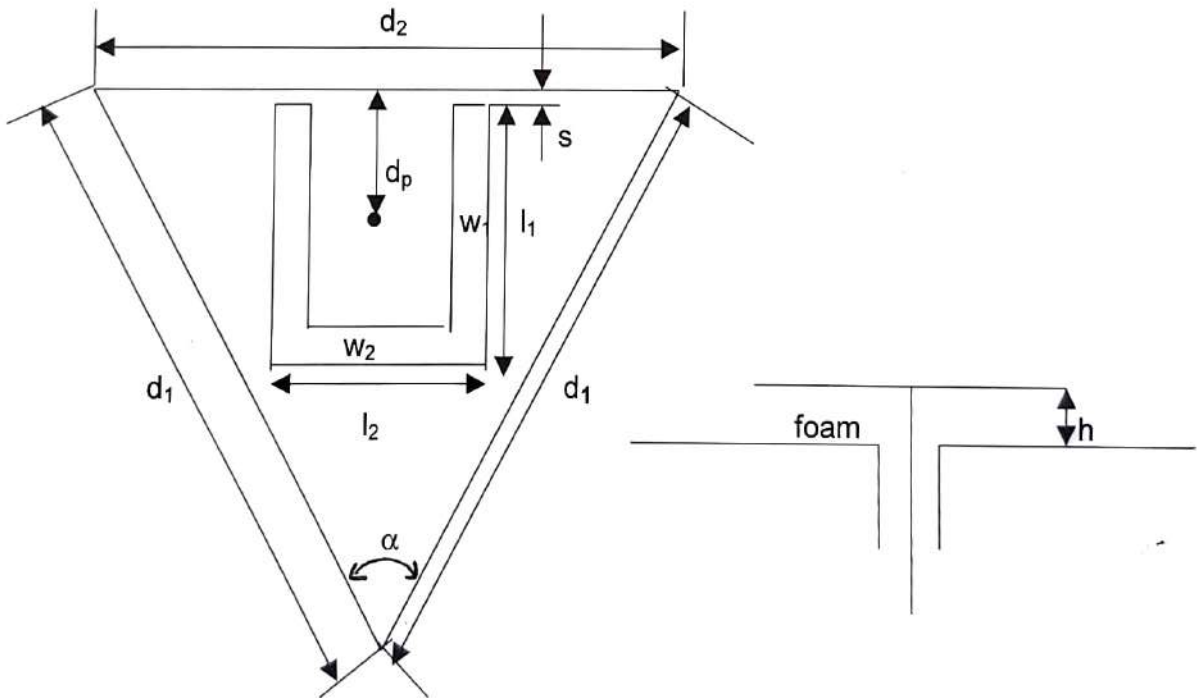


Fig. 4.1 Geometry of a U-slotted TMSA

The patch is mounted on a foam substrate ( $\epsilon_r = 1.01$ ) of thickness 14.3 mm ( $\sim 0.08 \lambda_0$ ). The antenna is fed by a  $50 \Omega$  coaxial probe of inner diameter of 2mm, close to the null-voltage point for the  $TM_{10}$  mode (the fundamental mode) of the patch without the slot.

### 4.3 Simulation results

The input impedance locus of the TMSA is shown in Fig. 4.2. Fig. 4.3 shows the VSWR plot against frequency for the same antenna. The bandwidth (VSWR = 2) is 20.8% which is approximately 2.0 times that of a corresponding un-slotted TMSA. It is also seen that the large inductive reactance component of the input impedance for a probe feed associated with a thick substrate is compensated by the capacitive reactance introduced by the U-slot. The broadside gain is plotted against frequency in Fig. 4.4. The maximum broadside gain is 8db at 16.5GHz. Figs. 4.5 to 4.7 shows the radiation patterns in the H-plane and E-plane at three frequencies. In both of the principal planes, the maximum cross-polarization is  $-10$  decibels for all frequencies. The half power beamwidths in the E-plane and H-plane are about  $60^\circ$  at all frequencies. There is no switch of polarization unlike U-slotted RMSA, as the two resonant modes are of the same polarization planes.

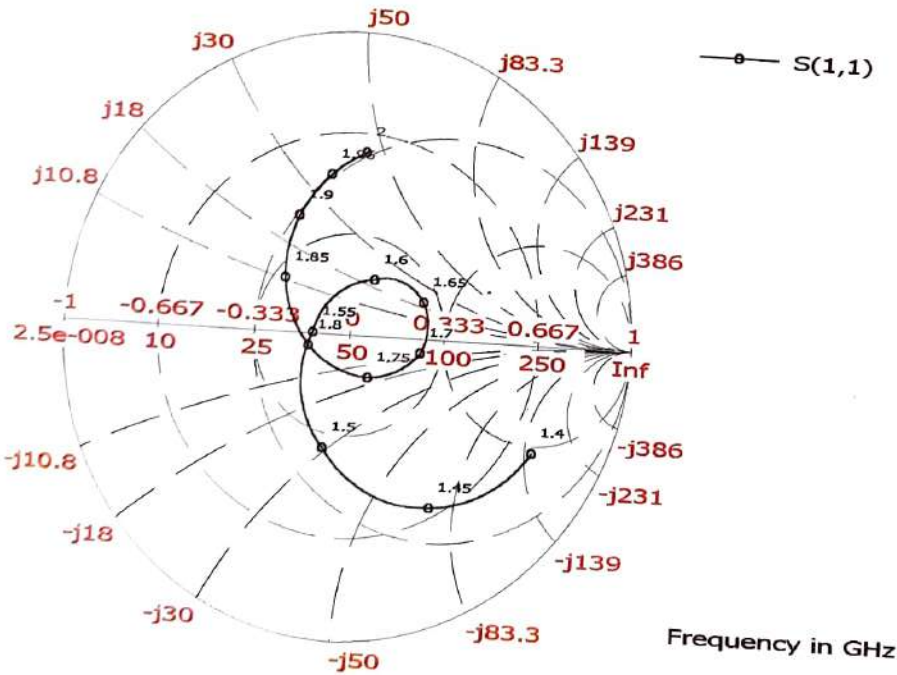


Fig. 4.2 Input impedance locus of U-slot TMSA

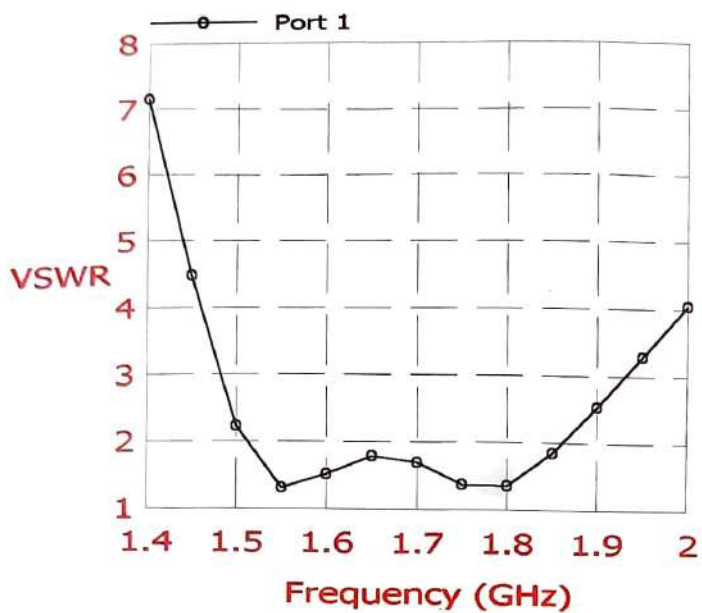


Fig. 4.3 VSWR vs frequency for U-slot TMSA

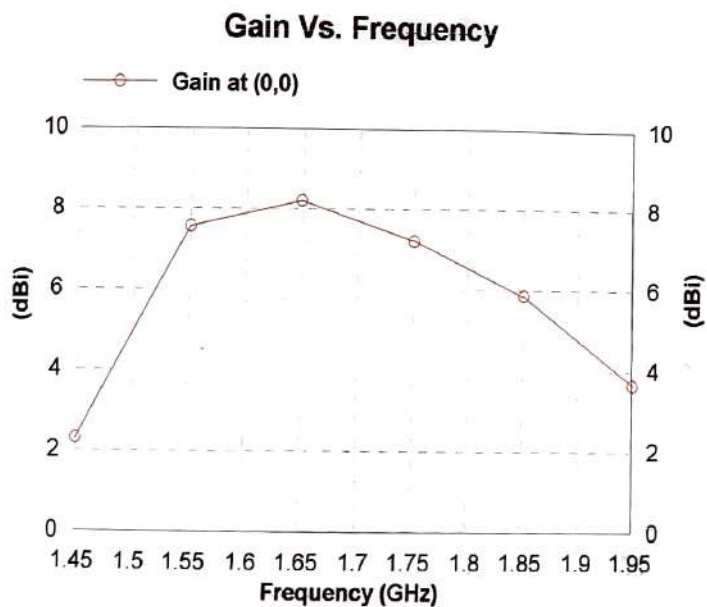


Fig. 4.4 Broadside gain against frequency for U-slot TMSA

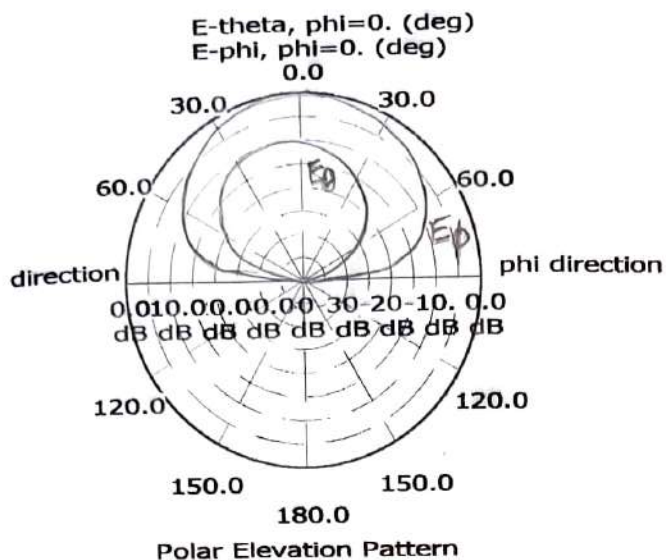
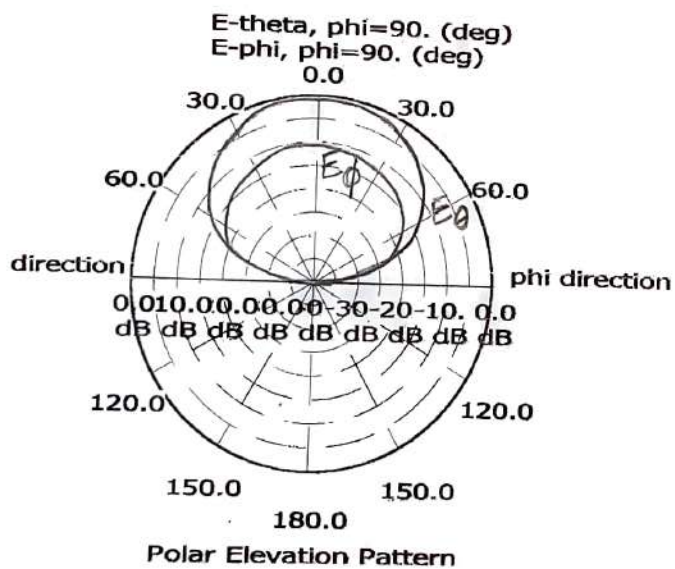
(a)  $\phi = 0^\circ$ (b)  $\phi = 90^\circ$ 

Fig. 4.5 Radiation patterns at 1.55 GHz (a) H-plane (b) E-plane

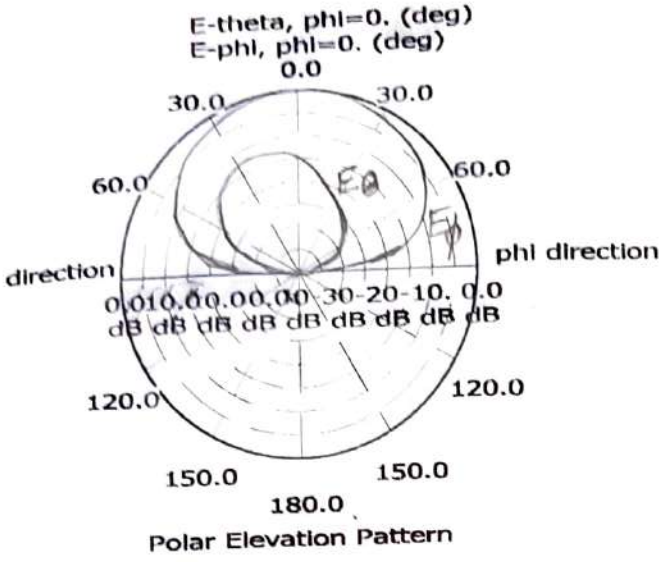
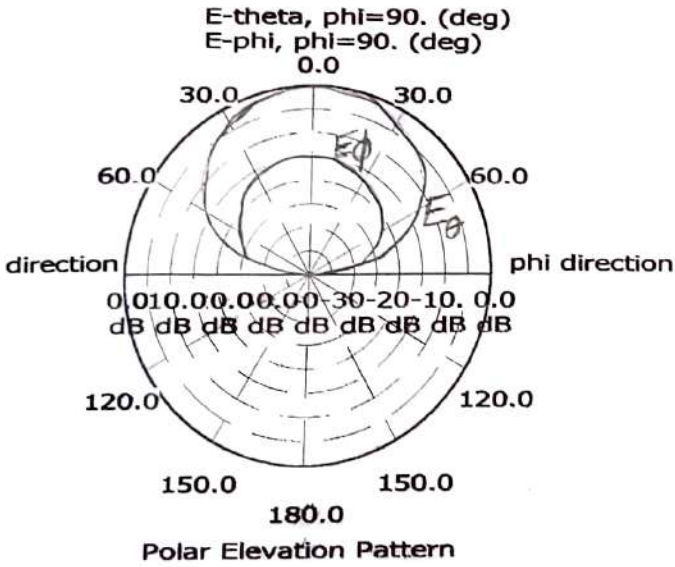
(a)  $\phi = 0^\circ$ (b)  $\phi = 90^\circ$ 

Fig. 4.5 Radiation patterns at 1.70 GHz (a) H-plane (b) E-plane



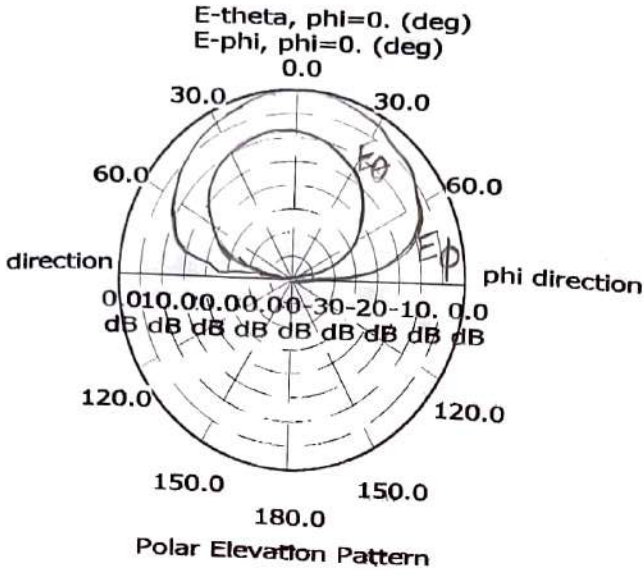
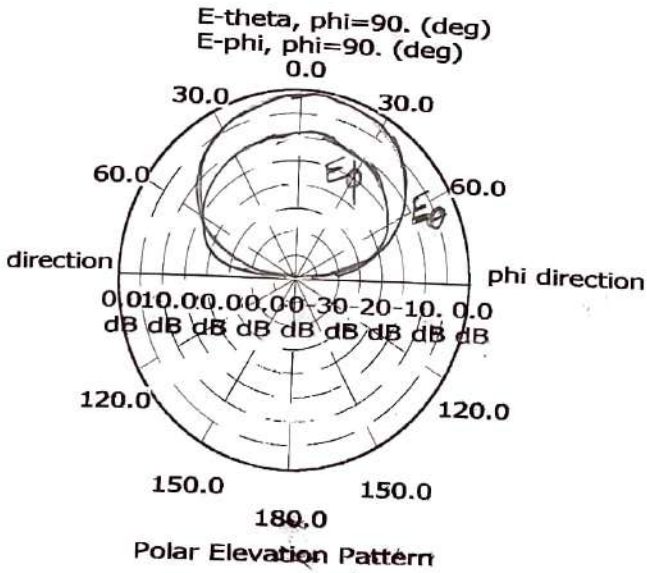
(a)  $\phi = 0^\circ$ (b)  $\phi = 90^\circ$ 

Fig. 4.6 Radiation patterns at 1.85 GHz (a) H-plane (b) E-plane

## Chapter 5

# Experimental and simulation studies of WLL and GSM frequency band U-slot RMSA

## 5.1 Introduction

An antenna which can work both in WLL and GSM frequency bands is designed, fabricated and tested. Dimensions of the WLL and GSM band U-slot RMSA in mm. is shown in table 4.1.

Table 5.1 Dimensions of the antenna in mm. (Refer to Fig. 2.1 for antenna geometry)

U-slot RMSA	W	L	F	$W_s$	$L_s$	a	b	c
Antenna A	241.68	128.3	66.15	55.38	95.38	11.54	21.38	10.1
Antenna B	181.68	128.3	66.15	55.38	95.38	11.54	21.38	10.1

The antenna has two layers of substrate as shown in Fig. 5.1. There is an air gap of 28.03 mm. and on the top of this, there is a layer of glass-epoxy ( $\epsilon_r = 4.3$ ) of 1.59 mm.

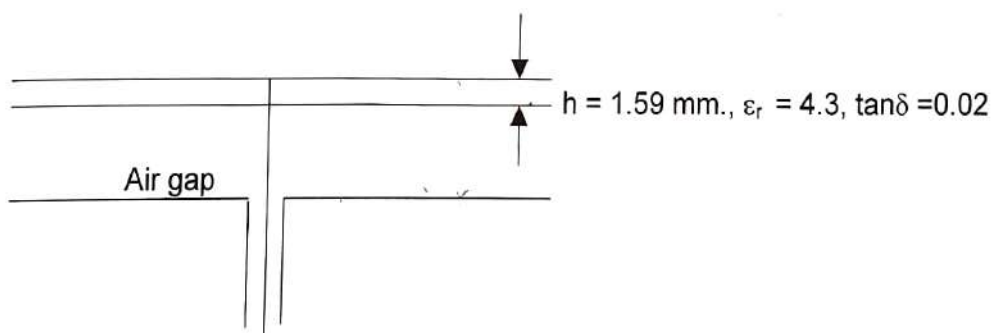
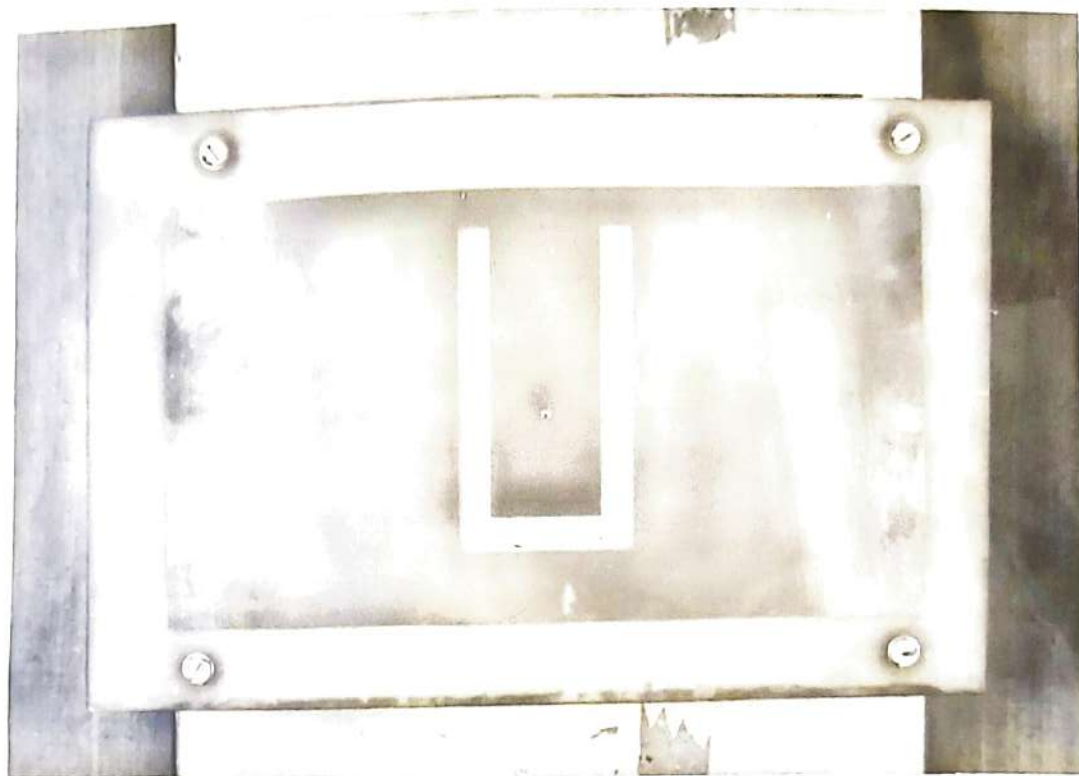


Fig. 5.1 Side view of antenna

The photograph of the antenna is shown in Fig. 5.2. The antenna is designed for a coaxial probe (N-type connector) of inner diameter 4mm. The experiment is done by mounting a wire of 2 mm. diameter on the N-type connector.



**Fig. 5.2 Photograph of the WLL and GSM band U-slot RMSA.**

## **5.2 Experimental and simulation results**

IE3D simulation results of the antenna are shown in Figs. 5.3 to 5.7. Fig. 5.3 shows that as we decreased the inner diameter of the coaxial probe from 4 mm to 2 mm, the input impedance of the antenna A has become more inductive. The antenna A has a bandwidth of 27.7%, from 0.72GHz to 0.95GHz, centered at 0.81GHz. The optimum case is achieved when the width of the antenna A is decreased 30mm from both sides (Antenna B) as shown in table 5.1. It gives a wider bandwidth from 0.725 GHz to 1 GHz of about 30% as seen from Fig 5.4. One more advantage of this is that higher order mode is suppressed thereby it gives a better pattern characteristics than the antenna A. The antenna B does not show switch of polarization. The decrease in broadside gain with frequency for antenna A in Fig. 5.9 and radiation pattern at 0.95 GHz in Fig. 5.8 shows switch of polarization. Fig. 5.10 shows the two cases where experimental results are taken using two wires of different diameters. For a wire of 1 mm. diameter shows a higher inductive component in the input impedance than the wire

of 2mm diameter which is in agreement with theoretical result. The experimental results are taken using HP Network Analyzer.

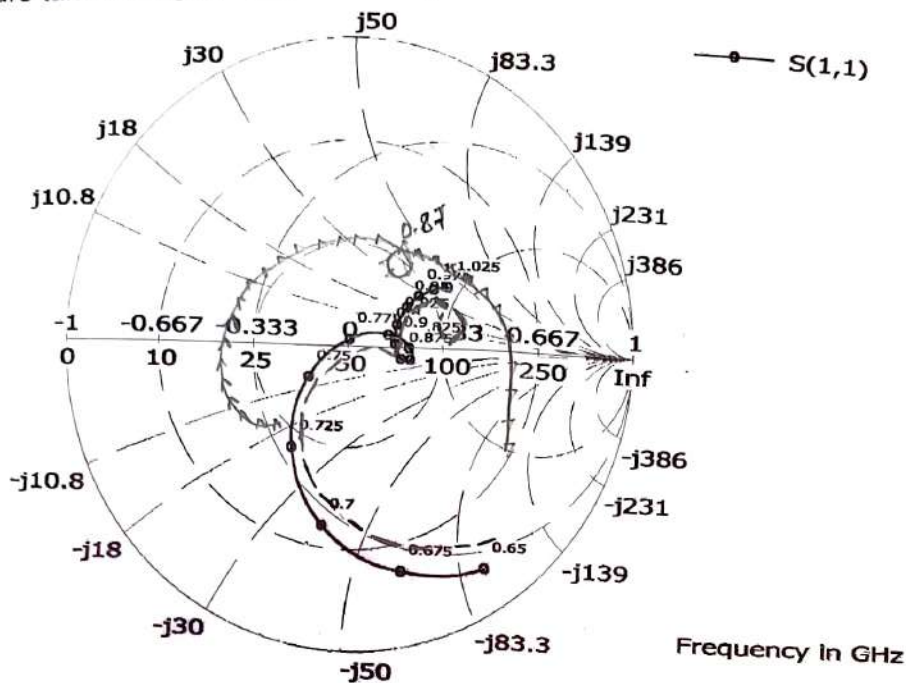


Fig. 5.3 Input impedance loci of WLL and GSM band U-slot RMSA. ( — ) Antenna B, ( - - - ) Antenna A, ( ····· ) Antenna A with coaxial probe of inner diameter 2 mm.

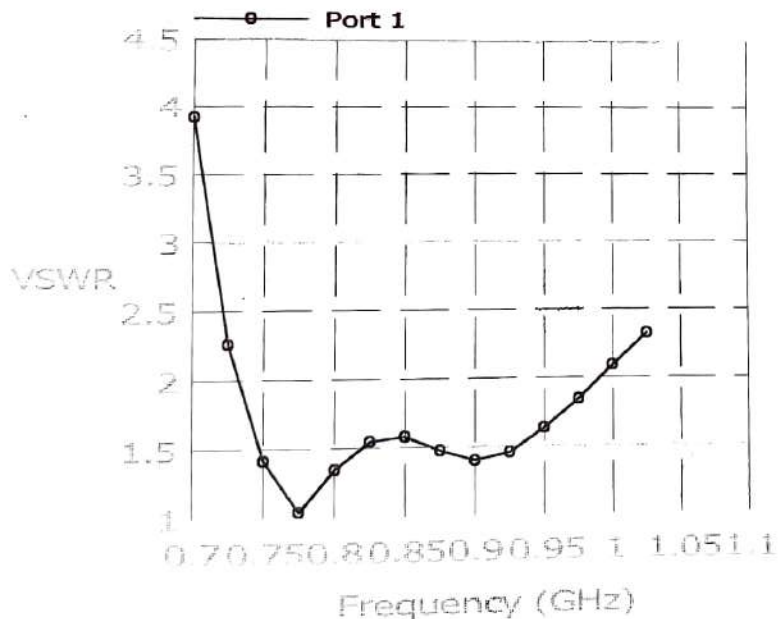


Fig. 5.4 VSWR vs frequency for WLL and GSM band U-slot RMSA (Antenna B).

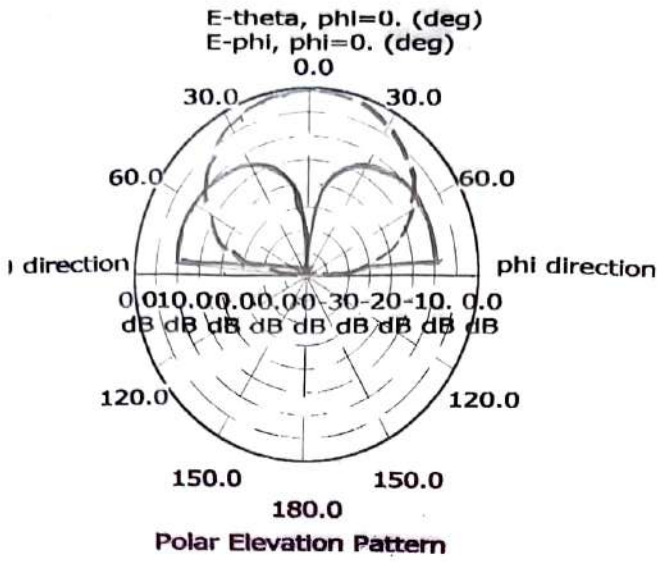
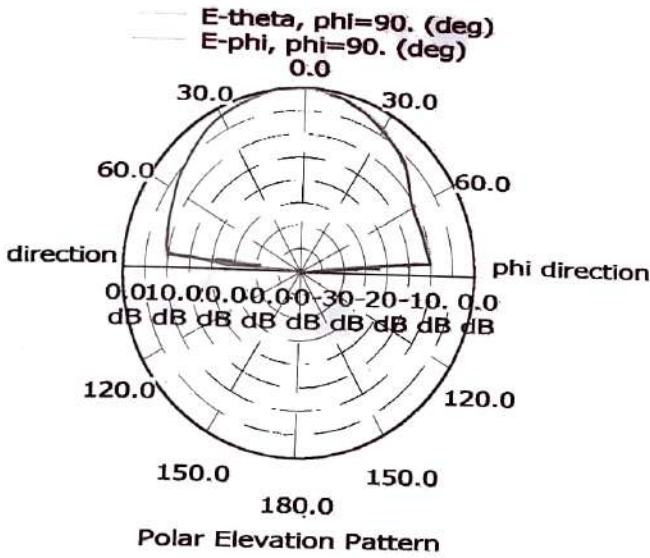
(a)  $\phi = 0^\circ$ (b)  $\phi = 90^\circ$ 

Fig. 5.5 Radiation patterns for Antenna B at 0.75GHz (a) H-plane (b) E-plane.

(—)  $E_\theta$ , (----)  $E_\phi$

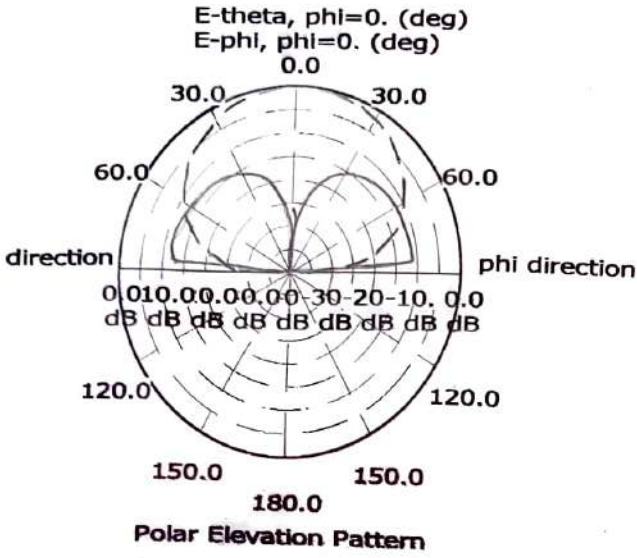
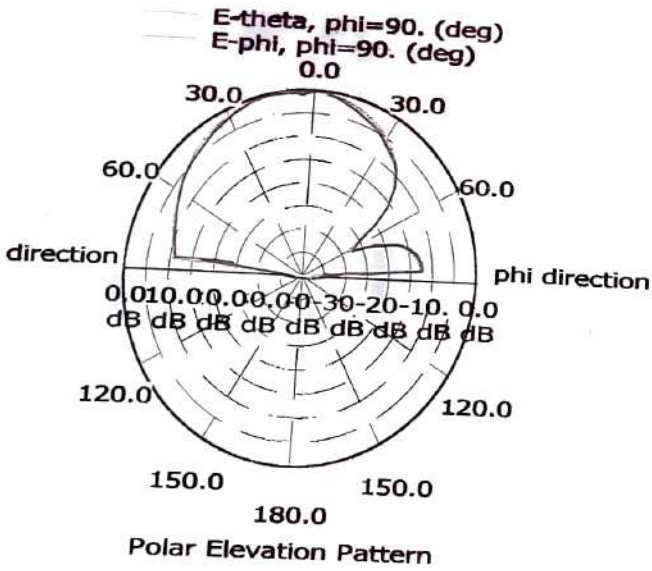
(a)  $\phi = 0^\circ$ (b)  $\phi = 90^\circ$ 

Fig. 5.6 Radiation patterns for antenna B at 0.85GHz (a) H-plane (b) E-plane.

( — )  $E_\theta$ , ( - - - )  $E_\phi$ .

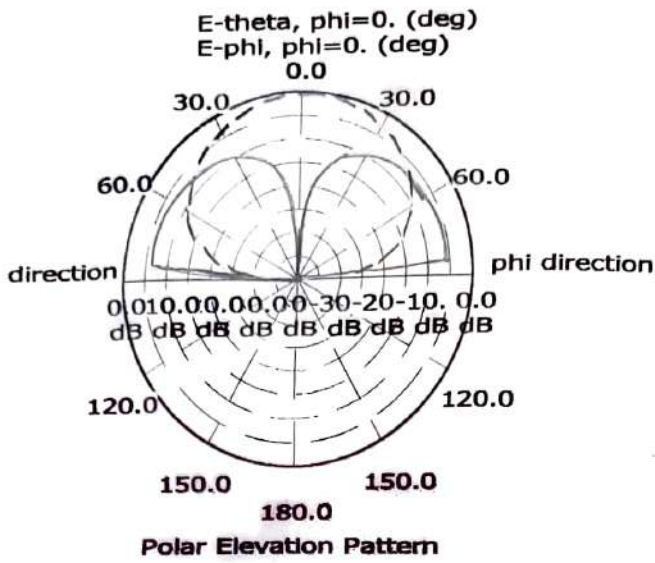
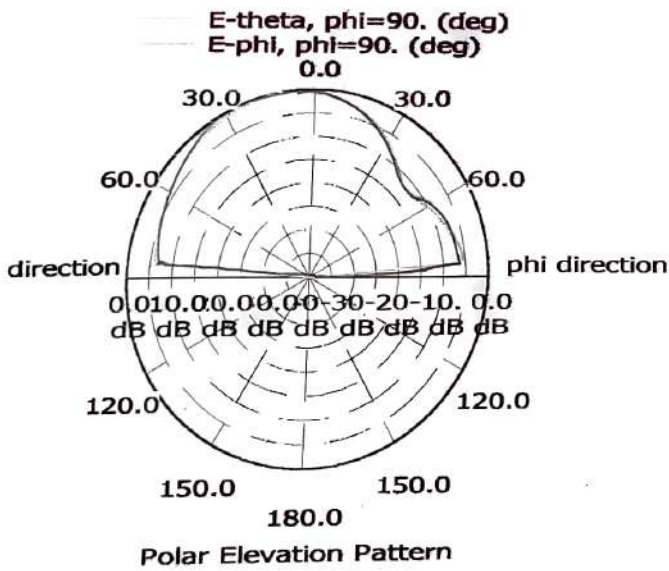
(a)  $\phi = 0^\circ$ (b)  $\phi = 90^\circ$ 

Fig. 5.7 Radiation patterns for Antenna B at 0.95GHz (a) H- plane (b) E-plane.

( — )  $E_\theta$ , ( - - - )  $E_\phi$ .

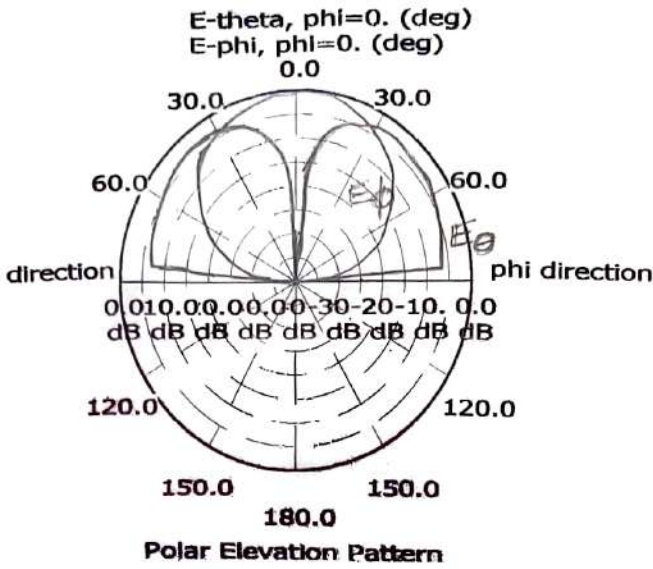
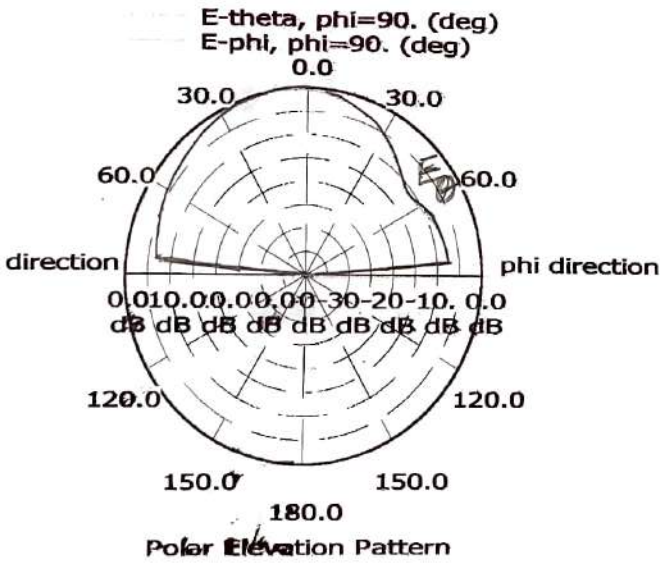
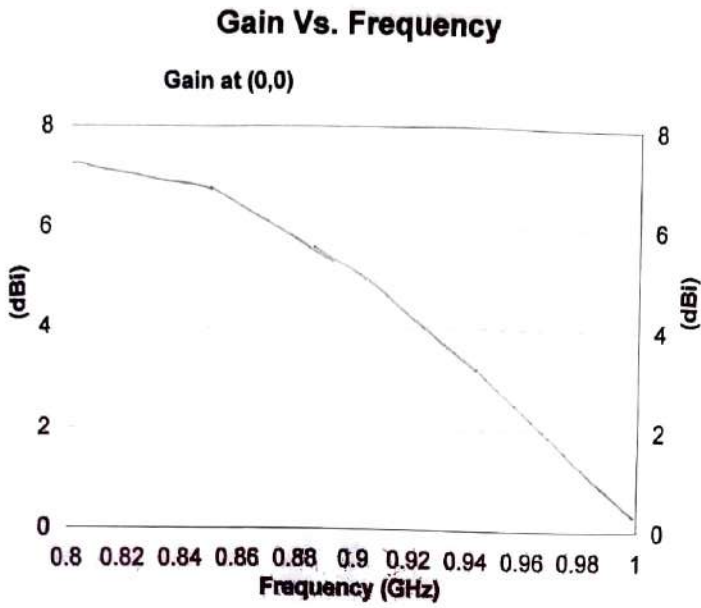
(a)  $\phi = 0^\circ$ (b)  $\phi = 90^\circ$ 

Fig. 5.8 Radiation pattern of Antenna A at 0.95 GHz (a) H-plane (b) E-plane





(a)

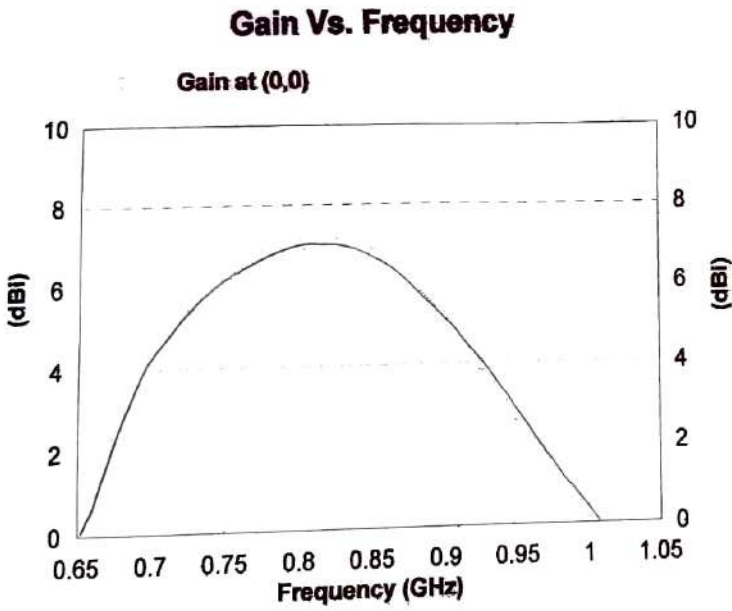
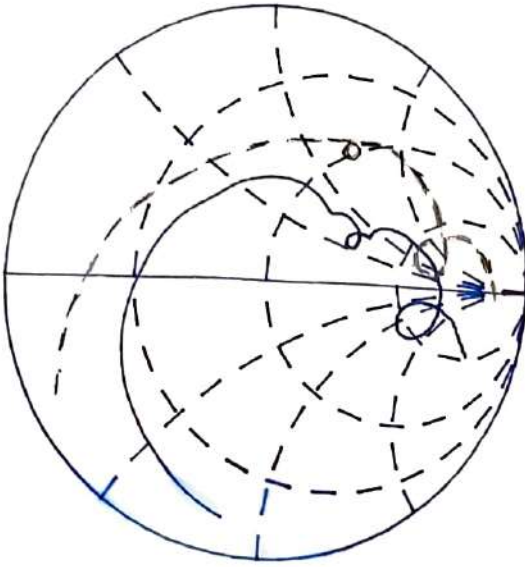
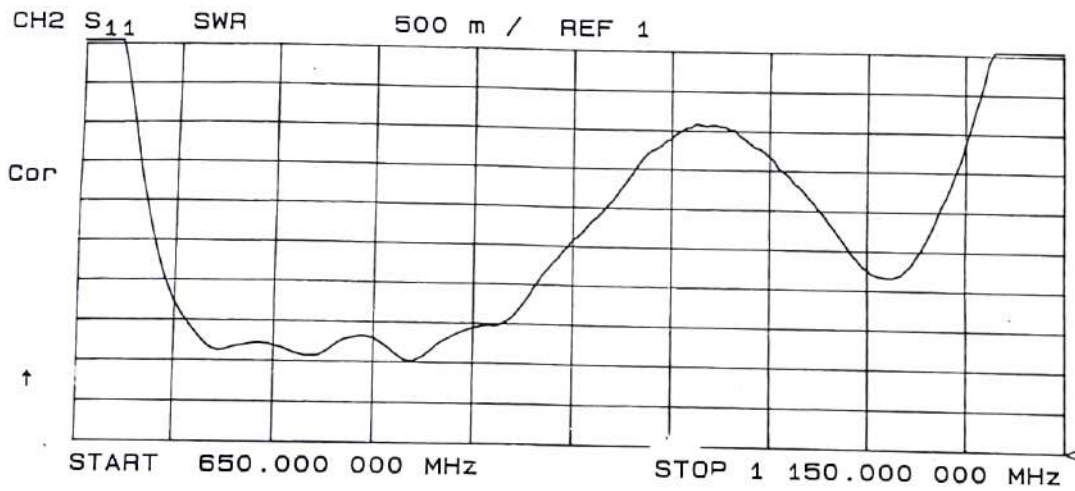


Fig. 5.9 Broadside gain vs frequency for (a) Antenna A and (b) Antenna B



(a)



(b)

Fig. 5.10 (a) Measured input impedance loci and (b) Measured return loss of Antenna A when diameter of the wire mounted on N-type connector is (—) 2mm and (- - -) 1 mm.

## Chapter 6

### Conclusion

#### 6.1 Conclusion

Microstrip antennas are low-profile, conformable to planar and non-planar surfaces, simple and inexpensive to manufacture using modern printed-circuit technology, mechanically robust when mounted on rigid surfaces, compatible with MMIC designs. Major operational disadvantage of MSA is its very narrow frequency bandwidth.

A brief literature survey on the various methods of bandwidth enhancement reveals that most of the techniques either increases the lateral size or thickness of the antenna. A U-slot MSA is compact, broad band and low-profile.

The effect of changing the slot dimensions on the antenna performance is studied. It shows that the notch resonant frequency is dependent on the physical length of the slot.

An additional U-slot on the RMSA further enhances the bandwidth. It is due to the additional notch resonant frequency introduced by the second U-slot. Switch of polarization due to the excitation of orthogonal modes is visible at the higher operating frequencies.

A U-shaped slot on TMSA gives a broadband with good pattern characteristics. It has the advantage of being smaller size than the corresponding RMSA with a U-slot. Unlike the latter antenna, it does not show switch of polarization.

A U-slot RMSA which can work both in WLL and GSM frequency band has been designed and studied experimentally.

To sum up, the following conclusion has been drawn from the project works:

- 1) It is found that a properly designed U-slot patch can exhibit wideband properties for RMSA and TMSA.
- 2) A RMSA with single U-slot has two adjacent resonant frequencies. The notch resonant frequency is dependant on the physical length of the U-slot.
- 3) The U-slot appears to introduce a capacitive component in the input impedance of the antenna thereby counteracting the inductive component of the coaxial probe.
- 4) For a double U-slot RMSA, an additional resonator is introduced by the additional U-slot thereby further enhancing the bandwidth of the antenna.
- 5) In RMSA with single or double U-slot, the antenna polarization can switch due to excitation of orthogonal modes. So, special care must be taken in the design to maintain the same polarization characteristics over the wide bandwidth.

## 6.2 Further investigation

In this project, an extensive study of the U-slot MSA has been done. Following points are suggested for further investigations:

- 1) The WLL\_GSM U-slot RMSA can be further optimized experimentally and theoretically.
- 2) Unlike other cases of changing slot dimensions of the U-slot, changing slot width does not follow the usual rule. That is, even if the slot width increase cause in the increase of total U-slot length, its effect on the input impedance is far more pronounced than the other cases. So, it needs to be further investigated.

## References

- [1] L. V. Blake, *Antennas*, John Wiley and Sons, 1987.
- [2] D. M. Pozar and D. H. Schaubert, *Analysis and design of microstrip antenna arrays*, IEEE press, 1995.
- [3] R. C. Johnson and H. Jasik, *Antenna Engineering Handbook*, Mcgraw-Hill Book Company, 1981.
- [4] C. A. Balanis, *Antenna theory, analysis and design*, Wiley and Sons, 1997.
- [5] N. Fayyaz and S. S.-Naeini, " Bandwidth enhancement of a rectangular microstrip antenna by integrated reactive loading, " *IEEE AP- Symposium Digest*, vol.-2, pp 110-1103, June 1998.
- [6] S. K. Palit and et al, " Design of a wideband dual- frequency notched microstrip antenna," *IEEE AP-Symposium Digest*, vol.-4, pp. 2351-2354, 1998.
- [7] S. K. Palit and A. Hamadi, "Design and development of wideband and dual-band microstrip antennas," *IEE Proc. Microw. Ant. Propagat.*, vol.-146, pp. 35-39, Feb. 1999.
- [8] R. Q. Lee and K. F. Lee, " Characteristics of a two-layer electromagnetically coupled rectangular patch antenna," *Electronic Letters*, vol.-23, pp. 1070-1072, Sept. 1987.
- [9] B. Barilese and C. Peiexiro, " Wide-band microstrip patch element," *IEEE AP-Symposium Digest*, vol.- 2, pp. 1104-1107, June 1998.
- [10] K. P. Ray, " Broadband, dual frequency and compact microstrip antennas," *Ph.D. Thesis, I.I.T-Bombay*, 1999.
- [11] T. Huynh and K. F. Lee, " Single-layer single-patch wideband microstrip antenna," *Electronic Letters*, vol.-31, pp. 1310-1312, Aug. 1995.
- [12] IE3D manual, *Zeland Software manual*, Zeland Software Inc., California, U.S.A.
- [13] Lee and et al, " Experimental and simulation studies of the coaxially fed U-slot rectangular patch antenna," *IEE Proc. Microw. Ant. propagat.*, vol.-144, pp. 354-358 oct. 1997.

- [14] Gou and et al, " Double U-slot rectangular patch antenna," *Electronic Letters*, pp. 1805-1806, Sept. 1998.
- [15] M. clenet and L. Shafai, " Multiple resonances and polarization of U-slot patch antenna," *Electronic Letters*, vol.-35, pp. 101-103, Jan. 1999.
- [16] K.-L. Wong and W.-H. Hsu, " Broadband triangular microstrip antenna with U-shaped slot," *Electronic Letters*, vol.-33, Dec. 1999.
- [17] K. F. Lee and W. Chen, *Advances in microstrip and printed antennas*, John Wiley and sons, 1997.
- [18] D. J. Griffiths, *Introduction to Electrodynamics*, Parentice-Hall, 1995.
- [19] K. Hirasawa and M. Haneishi, *Analysis, design and measurement of small and low profile antennas*, Artech House.
- [20] J. R. James and P. S. Hall, *Handbook of Microstrip Antennas*, vol. 1, Peter Peregrinus Ltd. 1989.
- [21] I. J. Bahl and P. Bhartia, *Microstrip antennas*, Artech House, 1980.

## Appendix

### A.1 Inductance of a coaxial cable

A long coaxial cable carries current  $i$  (the current flows down the surface of the inner cylinder, radius  $a$ , and back along the outer cylinder, radius  $b$ ) as shown in Fig. A.1.

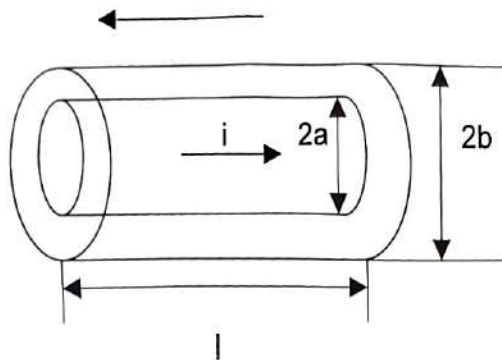


Fig. A.1 Coaxial cable

According to Ampere's circuital law, the field between the cylinders is

$$B = \mu_0 i / 2\pi r \quad (\text{A.1})$$

Elsewhere, the field is zero. Thus, the energy per unit volume is

$$\frac{1}{2} \mu_0 \left( \frac{\mu_0 i}{2\pi r} \right)^2 \quad (\text{A.2})$$

The energy in a cylindrical shell of length  $l$ , radius  $r$ , and thickness  $\delta r$ , then is

$$\left( \frac{\mu_0 i^2}{8\pi^2 r^2} \right) 2\pi r l \delta r \quad (\text{A.3})$$

Integrating from  $a$  to  $b$ , we have

$$\begin{aligned} W &= \mu_0 i^2 l / 4\pi \ln(b/a) \\ &= (1/2) L i^2 \end{aligned} \quad (\text{A.4})$$

or,

$$L = \mu_0 l / 4\pi \ln(b/a) \quad (\text{A.5})$$